Master Thesis GEO 511

August 2015

# Transformation and stabilization of Norway spruce needle-derived material in alpine soils during a one-year experiment: a $^{13}$C-labeling approach


Supervisor and faculty member:

Prof. Dr. Markus Egli

Co-supervisor:

Dr. Samuel Abiven

Marta Petrillo

Geochronology, Physical Geography Division

Department of Geography, University of Zurich

Author:

Simon Hafner

Buhnrain 6

8052 Zürich

simonhafner@access.uzh.ch

08-919-912

## Abstract

Large amounts of the terrestrial carbon reside in soil organic matter (SOM). The present work focuses on the influence that aspect and elevation have on the decomposition and stabilization of (SOM) in Alpine environments. For that purpose, an experiment with artificially $^{13}C$ labeled Norway spruce needles (*Picea abies*) ($\delta^{13}C$= +43.4 ‰) was carried out along a climosequence (five north and five south-exposed sites between 1200 and 2400 m a.s.l.) in the Northern Alps of Italy (Province of Trentino). The $^{13}C$ labeled needle substrate was exposed to natural decomposition during one year. Thereafter, the substrate recovery (as an indicator for SOM decomposition) was determined, based on the isotopic signatures of the labeled soil samples and related control soil. The resulting $^{13}C$ recoveries of the bulk soil amounted on average to 21.2 ± 7.9 % at the northern altitudinal sequence and to 34.1 ± 4.8 % at the southern elevation gradient. Furthermore, a density fractionation was carried out in order to investigate the potential stabilization of the applied substrate in two soil compartments. Thus, two soil fractions were separated by means of a Sodium Polytungstate density solution (1.6 g $cm^{-3}$). Thereof, a light fraction (LF) of ≤1.6 g $cm^{-3}$ (treated with ultrasound) and a heavy fraction (HF) of ≥1.6 g $cm^{-3}$ resulted. The density fractions were characterized by increasing $\delta^{13}C$ and $\delta^{15}N$ signatures with increasing particle density. At the northern gradient, on average 13.0 ± 4.0 % of the initial substrate was recovered in the LF and 9.1 ± 3.0 % in the HF. The southern gradient was characterized by mean substrate recoveries of 25.2 ± 4.0 in the LF and 8.2 ± 2.2 % in the HF. Furthermore, the results of the present work show that temperature and precipitation can distinctly alter soil properties as well as SOM decomposition and stabilization in alpine environments.

## Table of contents

## Table of figures

## Table of tables

# 1 Introduction

Within the current discussion about the world wide climate change and global warming, soil plays an important role in the biogeochemical carbon cycle, mainly due to the important carbon and nutrients storage potential of the soil (Egli et al., 2009). Schmidt et al. (2011) state that "globally, soil organic matter (SOM) contains more than three times as much carbon as either the atmosphere or terrestrial vegetation". Nevertheless, it is still unknown why some SOM are preserved in soil for millennia and other SOM decompose rather quickly (Schmidt et al., 2011).The quantification of SOM on a regional scale is important in order to provide essential information about the global biogeochemical carbon cycle, mainly to predict possible future feedback mechanisms in response to global climate change (Dahlgren et al., 1997). Beside the $CO_2$ sequestration in SOM, the investigation of SOM dynamics is necessary for the correct understanding of many functions and processes of the ecosystem.

SOM is the result of net fluxes into and out of the soil (Kammer and Hagedorn, 2011). These biologically regulated fluxes mainly depend on the primary production and SOM decomposition. Both processes are strongly influenced by climatic conditions. Biomass production and biological activity respond to temperature and precipitation changes (Davidson and Janssens, 2006; Garcia-Pausas et al., 2007). Furthermore, it is of interest which factors are responsible for holding soil organic carbon (SOC) in the SOC pool. Conceptual models assume that the stabilization of organic carbon (OC) is achieved through physical and chemical protection of SOM in different density fractions (Davidson and Janssens, 2006; Schmidt et al., 2011). The isolations of SOM from decomposers can be summarized as physical and chemical stabilization of SOM in soil (Bird et al., 2008; Schmidt et al., 2011; Schrumpf et al., 2013). Hence, it is of great interest to identify and quantify SOM decomposition and stabilization processes and their sensitivity to changing climatic conditions.

Forests store about 50% of the carbon in the terrestrial biosphere and therefore they represent a large carbon pool in the global carbon cycle, although they cover only 30% of the earth's land surface (Malhi, 2002). A significant portion of the forest's carbon exists as coarse woody debris (CWD) from dead trees and can amount up to 20% of the total carbon found in old grown forests (Harmon et al., 1986; Weedon et al., 2009). Although forests are considered to be large carbon pools, the processes and factors controlling CWD decomposition are poorly understood (Weedon et al., 2009). However, empirical studies have reported that local conditions such as temperature and humidity mainly control CWS decomposition (Kueppers and Harte, 2005; Weedon et al., 2009). Nevertheless, other studies additionally revealed that also plant species-specific characteristics alter the wood debris decomposition (Weedon et al., 2009). Therefore, it is interesting to look at how far forests and CWD function as a terrestrial carbon sink and whether climatic conditions and species-specific characteristic alter CWS decomposition (Kueppers and Harte, 2005).

Beside CWD dynamics plant litter deposition also represents an important nutrient flux of temperate forests and is often responsible for more than half of the annual carbon inputs into forest soils (Kammer and Hagedorn, 2011; Meentemeyer et al., 1982). Large amounts of the terrestrial net primary production take place in vegetation canopies. Depending on the plant species large amounts of the biomass are deposited annually as litterfall on the soil surface. Therefore, litterfall represents an important process in the organic carbon production-decomposition cycle (Meentemeyer et al., 1982). To what extent the deposited litter contributes to the soil carbon pool in the long term is mainly dependent on the mineralization rate of organic carbon to $CO_2$, the incorporation of organic

carbon into mineral soil by soil fauna and the leaching of dissolved organic carbon (DOC) (Kammer and Hagedorn, 2011). Additionally, litter quality, characterized by the C/N ratio and lignin concentration, can influence the litter decomposition rate in forests remarkably (Kammer and Hagedorn, 2011). Moreover, physical and chemical soil processes such as chemical binding of organic compounds to minerals or physical protection of SOC by aggregates formation are responsible for the stabilization of litter decomposition products in the soil (Davidson and Janssens, 2006; Schmidt et al., 2011). Furthermore, temperature and soil moisture also influence the litter decomposition considerably. Hence, climate change can alter the biogeochemical cycle by changing the biomass production, litter decomposition and stabilization processes in soil (Dahlgren et al., 1997; Liski et al., 2003). Therefore, local climatic conditions, litter quality, activity of soil organisms, physical and chemical protection of SOM mainly influence litter decomposition and stabilization in soils.

***D.A.CH-DecAlp***

In 2012 the DecAlp project started in the Italian Alps supported by the D.A.CH (Germany, Austria Confoederatio Helvetica) lead agencies Swiss National Science Foundation (SNSF), the Austrian Science Foundation (FWF) and the German Research Foundation (DFG). The abbreviation DecAlp refers to the proposed project to investigate the effect of climate on coarse woody debris ***Dec***ay dynamics in ***Alp***ine forested areas (DecAlp: www.decalp.org, access: 14.04.2015). The main objectives of this research program are to investigate the influence of deadwood properties and litterfall on forest ecosystems and carbon dynamics in alpine-forested areas as the sensitivity of SOM to environmental conditions is still poorly understood and detailed investigations are missing. Alpine areas were chosen due to the availability of stable SOM of very high ages while also very young SOM with reactive minerals are available. Furthermore, the researcher collective expects stronger effects of global warming on high-altitude ecosystems (DecAlp: www.decalp.org, access: 14.04.2015).

One of the four research core themes under the lead of Dr. Paolo Cherubini and Prof. Markus Egli focuses on CWD characteristics with the aim to analyze:

- how climates affect coarse woody decay on alpine sites,
- what time scales are involved in the CWD decay of *Picea abies*
- how do they vary according to climate and how quickly is CWD (*Picea abies*) integrated into soil organic matter fractions

The research topics mentioned above were investigated in natural forest ecosystems of subalpine sites along an altitudinal gradient (climosequence) (DecAlp: www.decalp.org, access: 14.04.2015)

***Objectives***

The present master thesis is part of the research questions mentioned by the DecAlp project and investigates the decomposition and stabilization of Norway spruce needles (*Picea abies*) in alpine environment. The two main objectives of this thesis concern the transformation and stabilization of Norway spruce needles (*Picea abies*) in an alpine environment during a one-year experiment. Therefore, a tracer study with $^{13}C$ labeled Norway spruce needles was conducted in the Italian Alps. On the base of an isotopic analysis the litter decomposition and stabilization mechanisms of the Norway spruce needles were investigated.

According to Kammer and Hagedorn (2011) the amount of initial aboveground plant litter, which is incorporated into the soil carbon pool, depends on the SOM losses due to the mineralization of plant litter to $CO_2$ by soil organisms and dissolved organic carbon (DOC) losses. On the other hand, it is of

importance to quantify the decomposition products of the initial Norway spruce needles in different soil compartments. Density fractionation is a helpful procedure to analyze soil fractions and the interaction of organic matter with minerals and soil aggregates (Schrumpf et al., 2013). In the present work, two soil fractions were separated and analyzed for their organic carbon concentrations and $\delta^{13}C$ signatures, with the aim to identify and quantify parts of the original applied Norway spruce needles in these two fractions.

Since litter decomposition depends on climatic conditions, such as temperature and humidity (Liski et al., 2003), the sampling sites were chosen according to a climosequence in the Alps of northern Italy. A climosequence examines soils on a mountainside or a mountain range. Generally, air temperature becomes predictably cooler with increasing elevation while soil moisture and precipitation normally rise with increasing elevation (Schaetzl and Anderson, 2005). Such altitudinal transects help to analyze the influence of changing temperature and precipitation on soil formation (Dahlgren et al., 1997). Hence, an additional objective of this thesis was to investigate the effect of different elevations and aspects to the soils properties in the study sites. First of all, the goal was to assess measurements about soil temperature at all study sites with the purpose of finding elevation and exposition dependent patterns in the soil temperature. Based on this information, the soil samples were analyzed with the aim to work out differences in SOC concentrations and carbon stocks along the climosequence. In a further step the applied and recovered Norway spruce needles per sampling site as well as the results of the density fractionation are set into relation to the climosequence. This means working out elevation and exposition specific differences for light (LF) and heavy fraction (HF) as well as for Norway spruce needles recoveries in each fraction. The mentioned aims of my thesis lead to the following research questions:

- Are significant differences between SOC concentrations and SOC stocks in the climosequence (altitude and exposure) observable?
- What amount of the Norway spruce needle substrate is recovered along the climosequence?
- Are there significant differences in substrate recovery along the altitudinal gradient and between different aspects notable?
- Is the applied substrate detectable and stabilized within soil fractions?
- Is a priming effect, caused by the added needle substrate, detectable?

***Related works and difficulties***

In order to investigate SOM characteristics in alpine areas many studies have been conducted along altitudinal gradients around the globe. Therefore, considerable numbers of data concerning SOM concentrations and soil SOC stocks of alpine regions are available. Most of the studies focus on altitudinal gradients neglecting the influence of exposition on SOM characteristics (Dahlgren et al., 1997; Dalmolin et al., 2006; Djukic et al., 2010; Garten and Hanson, 2006; Garten et al., 2000, 1999; Hitz et al., 2001; Leifeld et al., 2009; Murphy et al., 1998; Schindlbacher et al., 2010). Only a few authors also took into account the effect of different expositions on SOM dynamics (Egli et al., 2009; Garcia-Pausas et al., 2007). The major challenge regarding these different studies about the characteristics of SOM at altitudinal gradients are varying natural conditions at each location such as different climatic conditions, varying parent material, climate-dependent plant species and study-depending gradients. As a consequence, one should consider potential differences in the study setup when comparing results from different study sites. Most of the studies mentioned assume that only altitude affects SOM characteristics and neglect influences caused by different expositions.

Therefore, the DecAlp study site consists of northern and southern exposed sites with the intention to distinguish between different SOC characteristics due to elevation and exposure. Furthermore, mountain areas show highly heterogeneous soil profiles as a result of local scale variability in the soil environment (Egli et al., 2009; Garcia-Pausas et al., 2007). Hence, SOC concentrations and SOC stocks can vary strongly between study sites, within a single altitudinal gradient or even at one individual sampling site.

An advantage of the DecAlp project is, that several scientists investigated in the same sites and conducted various experiments. Therefore, additional data are available. For example, Tommaso Bardelli examined the same DecAlp site with greater focus on SOC concentration and sampled 15 soil cores (0-15cm) per sampling site. Thus, it is possible to compare the present data with already existing measurements of the same site. However, the comparability of the measured soil samples is not always guaranteed since Tommaso Bardelli included the litter layer in his samples, whereas in the present study the litter layer was removed previously to the analysis of the soil samples. The intention behind this procedure was to examine the impact of the labeled substrate on the humus layer. Thus, the data of Tommaso Bardelli and the present data of this thesis are only relatively and not entirely comparable.

Concerning litter decomposition, many studies are available and the diversity of applied approaches is large. Kammer and Hagedorn (2011), for example, used $\delta^{13}C$ depleted beech litter to determine the litter decomposition rate. Bird et al. (2008) applied $\delta^{13}C$ and $\delta^{15}N$ enriched Ponderosa pine litter to temperate conifer forest soils in the Sierra Nevada. Garten et al. (2000) calculated the decomposition of organic litter through a $^{13}C/^{12}C$ ratio by means of measuring $\delta^{13}C$ values of fresh litter and SOM. In contradiction to the approaches using stable isotopes to determine the litter decomposition rate, Liski et al. (2003) and Murphy et al. (1998) applied litter bags to measure litter mass loss during one year, or two years respectively. However, the purpose of the present study is the application of $^{13}C$ labeled Norway spruce needle litter to all sampling sites (elevations and expositions) and to evaluate exposition and elevation specific SOM decomposition and stabilization.

# 2 Materials and methods

***Study area***

The study area is located in northern Italy in the province of Trentino. The sampling sites are distributed along several sites in and around Val di Rabbi (Fig. 1)

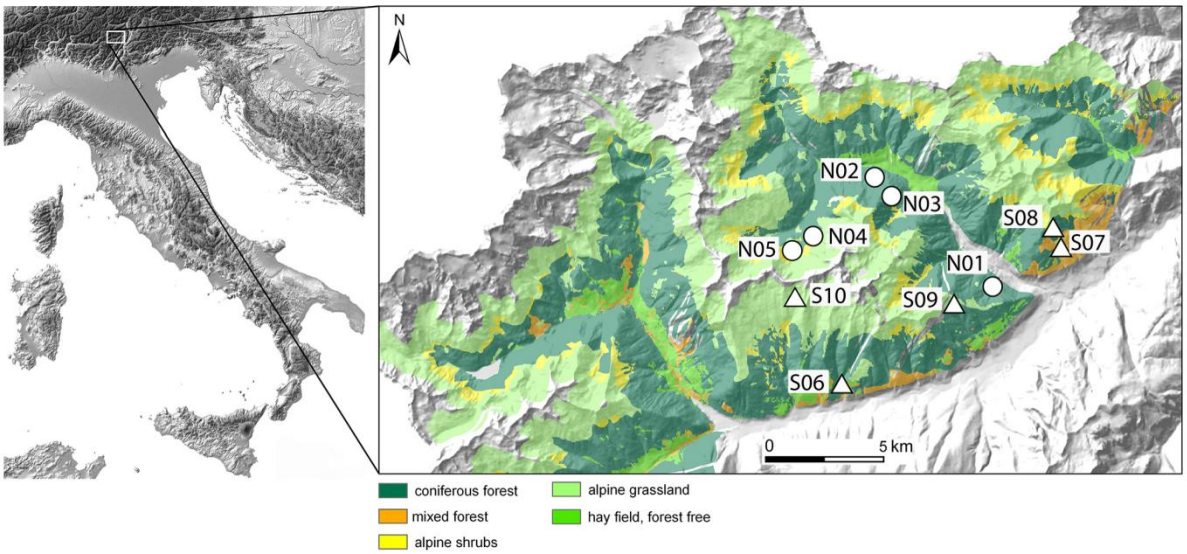


Fig. 1. Location of the study area and the sites in the province of Trentino (Petrillo et al., 2015).

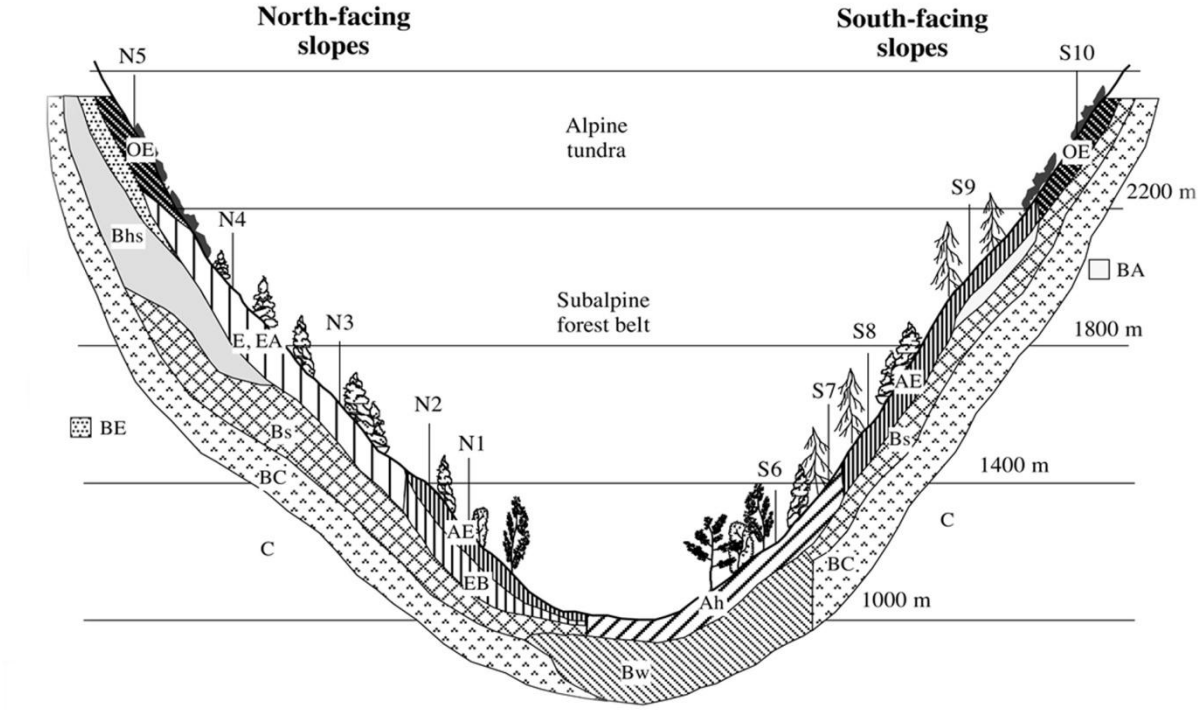


Fig. 2. Idealized altitudinal sequence of the sampling sites at five different elevations (Egli et al., 2006).

In total, the sampling area contains ten sampling sites. The sampling sites N01-N05 are located on north-facing slopes and the other five sites S06-S10 on south-facing slopes. Furthermore, all sites were distributed over an altitudinal gradient from 1200 to 2600 m a.s.l. (Egli et al., 2006). The sites N01 and S06 represents the two lowest and N05 and S10 the two highest located sampling sites (Fig. 1, Fig. 2, Table 1). Depending on the sampling site, three different soil types can be found: Cambisols,

Umbrisols, and Podzols. All sites have siliceous parent material, which consists of paragneiss (Egli et al., 2006). The sampling sites are characterized by a temperate (below the timber line) and alpine (above timber line) climate. The climate, measured at the neighboring village Peio (1580 m a.s.l.), show a mean annual temperature of 6.8°C and a mean annual precipitation of 861 mm $y^{-1}$ (Egli et al., 2006). Depending on the elevation, the sampling sites show different climatic conditions. The mean annual temperature and precipitation varies between the lowest and highest located sampling sites from 8.2 to 0°C and from 800 to 1300 mm $y^{-1}$ respectively (Egli et al., 2006).

Table 1
Characteristics of the study sites in Val di Rabbi (Egli et al., 2006)

| Profile | Elevation (m a.s.l.) | Aspect (°N) | Slope (°) | Parent material | Vegetation | Land use | WRB (1998) |
|---|---|---|---|---|---|---|---|
| North-facing-sites | | | | | | | |
| N1 | 1200 | 340 | 31 | Paragneiss debris | Abietetum albae | Natural forest (ecological forestry) | Chromi-Episkeletic Cambisol (Dystric) |
| N2 | 1400 | 0 | 28 | Paragneiss debris | Piceetum montanum | Natural forest (ecological forestry) | Chromi-Episkeletic Cambisol (Dystric) |
| N3 | 1650 | 0 | 29 | Paragneiss debris | Piceetum montanum | Natural forest (ecological forestry) | Chromi-Endoskeletic Cambisol (Dystric) |
| N4 | 1950 | 20 | 12 | Paragneiss debris | Nardetum alpigenum | Occasionally used as pasture | Episkeletic Podzol |
| N5 | 2400 | 30 | 25 | Paragneiss debris | Rhododendro-vaccinietum extrasilvaticum | Natural grassland and shrubs | Enti-Umbric Podzol (Episkeletic) |
| South-facing-sites | | | | | | | |
| S6 | 1200 | 160 | 31 | Paragneiss debris | Orno-ostryon | Ex-coppice, natural forest (ecological forestry) | Episkeleti-Endoleptic Cambisol (Chromi-Dystric) |
| S7 | 1400 | 145 | 33 | Paragneiss debris | Larix decidua | Natural forest (ecological forestry) | Dystri-Endoskeletic Cambisol |
| S8 | 1650 | 210 | 33 | Paragneiss debris | Larix decidua | Natural forest (ecological forestry) | Skeletic Umbrisol |
| S9 | 1950 | 160 | 25 | Paragneiss debris | Larix decidua/Picea abies | Ex-pasture, natural forest | Skeletic Umbrisol |
| S10 | 2400 | 190 | 28 | Paragneiss debris | Festucetum | Natural grassland | Dystri-Epileptic Cambisol |

***Experimental design***

At all ten sites four mesocosms (polyethylene tubes), each with a length of 20 cm and a diameter of 10 cm, were penetrated 15 cm into the soil (Fig 3).

Fig. 3. Mesocosms at the site N01 (©Marta Petrillo).

The mesocosms were inserted into the soil in summer 2012 and then let undisturbed for a period of one year. In June 2013, approximately 1.4- 2 g of $^{13}C$ labeled and milled Norway spruce needles substrate (*Picea abies*) was added to each mesocosms. During this process the litter layer was carefully removed and then the labeled material added and gently mixed with the upper soil layer. Afterwards the litter layer was placed back onto the soil. For that purpose, Norway spruce plants, which had been the source for the labeled spruce needles, were grown for four months in a $^{13}CO_2$ - enriched atmosphere in the MICE (Multi Isotopic labeling in a Controlled Environment) chamber at the University of Zurich. After four months, the spruce plants were harvested and dried. For the field experiment only the labeled needles were used. Therefore, the needles were simply collected after the harvesting period, milled and then the $\delta^{13}C$ signal measured. The measured $\delta^{13}C$ signal amounted to +43.4‰ and the organic carbon concentration of the needles accounted for 44.99 %. Close to the mesocosms the soil temperature was measured by means of miniature temperature loggers (iButton®) (Schmid et al., 2004) during the field application of the labeled substrate. The iButtons® were placed 10 cm below the soil surface. The soil temperature was measured between July 2013 and June 2014 in 3h steps. For the placement of the iButtons® and processing of the temperature data members of the DecAlp (www.decalp.org) team were responsible (Marta Petrillo and Dr. Kerstin Anschlag).

***Soil sampling and analysis***

One year after the labeled needles were added to the mesocosms, the mesocosms were excavated in July 2014, carefully sealed and then transported to the laboratory. Additionally, at each sampling site four soil replicates were excavated close to the mesocosms with a core driller as a means of obtaining 15 cm of control soil. In the laboratory, the samples were unsealed, the litter removed and then segmented into the sampling depths of 0-5 cm, 5-10 cm, and 10-15 cm. Afterwards, all samples were dried in the oven at 40°C for three days. The soil weight of all layers was measured before and after the drying period in the oven in order to obtain soil moisture at the day of sampling. By means of the dry weight and the dimensions of the mesocosms the bulk density (BD) of the samples was calculated. All samples were then sieved into factions of >2 mm and ≤2 mm. The fraction of >2 mm was weighed again in order to obtain the skeleton mass. The fraction of ≤2 mm was ball milled in a planetary mill. The milled fine earth fraction was used to measure C and N characteristics (CHN Analyzer: TruSpec Macro Analyzer) and the $\delta^{13}C$ signal of each sample with a Piccaro combustion module. On the fraction of ≤2 mm a density fractionation with two fractions was also carried out. Soil pH- value was determined in separate samples which were located near the mesocosms. The pH-values were measured in deionized water using a soil solution ratio of 2:20. Soil-pH measurements were conducted by Bardelli (2013).

***Density fractionation***

To separate the soil samples into two fractions a density fractionation was conducted. A "light fraction" (LF) and a "heavy fraction" (HF) were separated, the former with a density ≤1.6 g $cm^{-3}$ and the latter with a density >1.6 g $cm^{-3}$. The density of 1.6 g $cm^{-3}$ was chosen as a means of achieving an optimum density cut-off to obtain a LF with maximum organic and minimum mineral material in it (Cerli et al., 2012). In contrast to the investigations of Cerli et al. (2012) and Singh et al. (2014), the two light fractions (free light fraction and occluded light fraction) were not separated in the present investigation. The applied procedure is a simplified combination of the procedure employed by Christensen (1992) and Zollinger et al. (2013). For the density fractionation, dry soil material ≤2 mm was used. To achieve the density cut-off at 1.6 g $cm^{-3}$ a Sodium Polytungstate solution (SPT) was applied. In contrast to the procedure of Cerli et al. (2012) and Singh et al. (2014), the separation of the two fractions was done by centrifuging the fractions and not by filtering the fractions with a glass-fiber filter. Before the separation, 5 g of soil (fraction ≤2 mm) were mixed with 50 ml SPT solution of 1.6 g $cm^{-3}$ and then dispersed via ultrasound (Bandelin Sonoplus HD 3400; Berlin, Germany; calibrated according to (Schmidt et al., 1999)). Similar to Singh et al. (2014), 250 J $ml^{-1}$ of disruptive energy per sample were applied. After the ultrasonic treatment the samples were stirred for 1.5 h. Subsequently, the samples were centrifuged for 30 min with 3000 g (Heraeus Megafuge 1.0). The LF was then floating on top of the liquid and the HF was well settled on the bottom of the centrifugal tube. As a result, the supernatant LF was easily separable from the HF. All fractions were then rinsed with deionized water until the conductivity of the sample water solution was below 50 µS $cm^{-1}$. Subsequently all samples were dried in the oven at 40°C for 2 days. Then the final dry weigh was compared to the initial weight and the mass balance was calculated. Total C and N of all fractions as well as the $\delta^{13}C$ and $\delta^{15}N$ were measured by the Fodanzione Edmund Mach (FEM).

***Calculations***

Carbon stocks were calculated for the upper 15 cm according to the following equation:

$$C_{stocks} = \sum_{i}^{dz} c_i \rho_i d_i (1 - RM) \quad \text{(Zollinger et al., 2013)} \quad (1)$$

where $C_{stocks}$ connotes the carbon stocks over the indicated soil depths (kg $m^{-2}$), $c$ the organic carbon concentration (kg $t^{-1}$), $\rho$ the soil density (t $m^{-3}$), $d$ the thickness of the considered layers (m) and $RM$ the mass proportion of rock fragments per sampling layer (Zollinger et al., 2013).

To compare the $\delta^{13}C$ values between the control and labeled soil, a simple two-compartment model was applied. All observations and calculations assume that the $\delta^{13}C$ value of the soil is mainly influenced by the $\delta^{13}C$ value of the plant leaves, since plant leaves will be deposited and transformed to SOM at a later stage (Bernoux et al., 1998). The following equation represents the simple two-compartment model:

$$\delta^{13}C_{labeled\_soil} = \beta * \delta^{13}C_{substrate} + (1 - \beta) * \delta^{13}C_{control\_soil} \quad \text{(Bernoux et al., 1998)} \quad (2)$$

where $\delta^{13}C_{labeled\_soil}$ represents the $\delta^{13}C$ value of the mixture of the $\delta^{13}C$ values of the substrate and the control soil (‰), $\delta^{13}C_{substrate}$ the $\delta^{13}C$ signal of the substrate, $\delta^{13}C_{control\_soil}$ the $\delta^{13}C$ value of the control soil and β the proportion of organic carbon from the substrate compared to the OC of the control soil *(0-1)* (Bernoux et al., 1998). In this thesis, the formula (2) is interpreted as a unique pulse-labeling experiment where the labeled Norway spruce needles were applied to the soil with distinct enriched isotopic signature compared to the natural soil. Thereafter, the $\delta^{13}C$ signal theoretically peaked right after the application and afterwards decreased continuously with time due to mineralization of the labeled substrate by the soil fauna. After one year of field application the $\delta^{13}C$ labeled soil is characterized by a mixed signal composed of the initial $\delta^{13}C$ signal of the natural soil ($\delta^{13}C_{control\_soil}$) and of the added artificial $\delta^{13}C$ signal of the substrate ($\delta^{13}C_{substrate}$) relative to the factor time (Bernoux et al., 1998). The rearrangement of formula (2) allows calculating β starting from $\delta^{13}C_{control\_soil}$, $\delta^{13}C_{substrate}$ and $\delta^{13}C_{labeled\_soil}$ with the aim to determine the substrate recovery at a certain point of time (one year) during the decomposition of the artificial substrate:

$$sub\_rec = \frac{\delta^{13}C_{labeled\_soil} - \delta^{13}C_{control\_soil}}{\delta^{13}C_{substrate} - \delta^{13}C_{control\_soil}} * 100 \quad \text{(Bernoux et al., 1998)} \quad (3)$$

where *sub_rec* represents substrate recovery in percent.

A problem emerges from the fact that at the start of the labeling experiment the soil does not have the $\delta^{13}C$ signal of the substrate but rather a mixed $\delta^{13}C$ signal of the natural soil and the substrate. Therefore, the $\delta^{13}C$ signature of the labeled substrate is diluted by the natural $\delta^{13}C$ signature of the soil. This leads to an adaptation of the formula (3):

$$\alpha = \frac{c_{substrate} * m_{substrate}}{c_{substrate} * m_{substrate} + c_{control\_soil} * m_{control\_soil}}$$

$$1 - \alpha = \frac{c_{soil} * m_{soil}}{c_{substrate} * m_{substrate} + c_{control\_soil} * m_{control\_soil}}$$

$$\delta^{13}C_{t0} = \alpha * \delta^{13}C_{substrate} + (1 - \alpha) * \delta^{13}C_{control\_soil}$$

$$sub\_rec = \frac{\delta^{13}C_{labeled\_soil} - \delta^{13}C_{control\_soil}}{\delta^{13}C_{t0} - \delta^{13}C_{control\_soil}} * 100 \quad (4)$$

where *sub_rec* means substrate recovery in percent, *c* the SOC concentration of the indicated soil samples, *m* the mass of the mentioned samples and $\delta^{13}C$ the isotopic ratio of the indicated soil samples. $\delta^{13}C_{t0}$ represents the $\delta^{13}C$ signal resulting from the mixing of the substrate with the natural soil at the point of time ($t_0$) when the substrate was applied to the soil.

The priming effect was calculated according to the following equation:

$$PE = C_{label} - C_{control} \quad \text{(Fontaine et al., 2004)} \quad (5)$$

where *PE* means priming effect (g $kg^{-1}$), $C_{label}$ the SOC concentration of the labeled sample (g $kg^{-1}$) and $C_{control}$ the SOC concentration of the control sample (g $kg^{-1}$).

Error propagation was used to assess the standard errors of SOC stocks as site-specific mean values for bulk density were calculated. This procedure was necessary since the bulk density per sampling site significantly differed between the control samples, which were taken with a core driller, and the labeled samples obtained from the mesocosms. In order to calculate the error propagation the following equation was applied:

$$se_F = \sqrt{\left(\frac{\partial F}{\partial x}\right)^2 (se_x)^2 + \left(\frac{\partial F}{\partial y}\right)^2 (se_y)^2 + \left(\frac{\partial F}{\partial z}\right)^2 (se_z)^2} \quad \text{(Kragten, 1994)} \quad (6)$$

where $se_F$ represents the uncertainty of the final result of the function *F* and $se_x$, $se_y$ and $se_z$ the uncertainties of the each parameter.

Sensitivity analysis was applied to estimate the sensitivity of a dependent variable from an independent parameter described by the following equation:

$$Q_{i,m} = \frac{\partial \ln C_i}{\partial \ln P_m} \quad \text{(Egli and Fitze, 2001)} \quad (7)$$

where $Q_{i,m}$ indicates a change of 1% of the parameter $P_m$ on the output of the dependent variable $C_i$. Positive $Q_{i,m}$ indicates an increase in $C_i$ due to an increase in $P_m$ while negative $Q_{i,m}$ show a decrease in $C_i$ caused by an increase in $P_m$ (Egli and Fitze, 2001).

***Piccaro measurement and processing***

Since the upper 0-5 cm layer was highly organic it was not possible to process the raw data of the Piccaro measurements with the usually applied software correctly. Either the standard algorithm processed the samples with high organic carbon content wrong or no analysis of the raw data was possible. Therefore, a special R-script was used to process the raw data of the Piccaro measurements. The raw data from the Piccaro measurements were characterized by $CO_2$ concentration measurements in small time intervals (~1 sec steps). Hence, the raw data per analyzed sample were described as $CO_2$ data points per second and formed a bell-shaped curve with the $CO_2$ concentration on the y-axis and the time on the x-axis. Since the Piccaro is an automatic analyzer several samples were measured successively and saved as continuous data. Between two samples the $CO_2$ background in the Piccaro combustion chamber was always measured. For this reason, it was necessary that the R-script was able to separate different $CO_2$ bell curves of different samples in one file as well as to detect the starting and end point of the different bell curves of each sample. The latter was required in order to calculate the surface below the bell curve by numerical integration so that the total $CO_2$ released per sample was determinable. To define the starting point and end point of one bell curve of one sample, the first and second numerical derivation of the numerical bell curve was used. With two threshold values for the first and second numerical derivation it was possible to define the starting and endpoint of the bell curves very precisely. Afterwards, the integrated $CO_2$ bell curves were then linked with a regression to SOC contents of the samples. The exact R-code is displayed in the appendix.

***Statistical analysis***

All statistical analyses were performed using the software RStudios (RStudio v0.98.1103 – November 6th, 2014). To verify normal distribution of the samples a Shapiro Wilk test was conducted. If the test indicated a normal distribution of the samples then a t-test or an analysis of variance (ANOVA) were carried out, otherwise Mann-Whitney or Kruskal Wallis tests were used to statistically compare the samples. All statistical tests were carried out on a level of significance of 0.05. In order to enlarge the sample size the control and the labeled replicates per sampling sites were combined as long as the analyzed soil property was not influenced by the added substrate and no significant differences between control and labeled samples existed. This was the case for the SOC concentration, total nitrogen concentration, C/N ratio, SOC stocks, fraction-dependent mass distribution, fraction-dependent C and N distribution, fraction-dependent SOC concentration, fraction-dependent nitrogen concentration and the fraction-specific C/N ratio. When mean values were calculated the standard error was always used in order to indicate how precisely the sample mean value represents the population mean value.

# 3 Results

## 3.1 Bulk soil (0-15 cm)

***General soil properties***

The mean annual soil temperature varied at the northern gradient between 5 and 7.3 °C and at the southern gradient between 6 and 8.7 °C (Table 2). Both aspects exhibited decreasing mean annual soil temperatures with increasing altitude (Fig. 4). Overall, the north-facing sites showed distinctly (p=0.000, n=1459) lower soil temperatures than the south-exposed gradient.

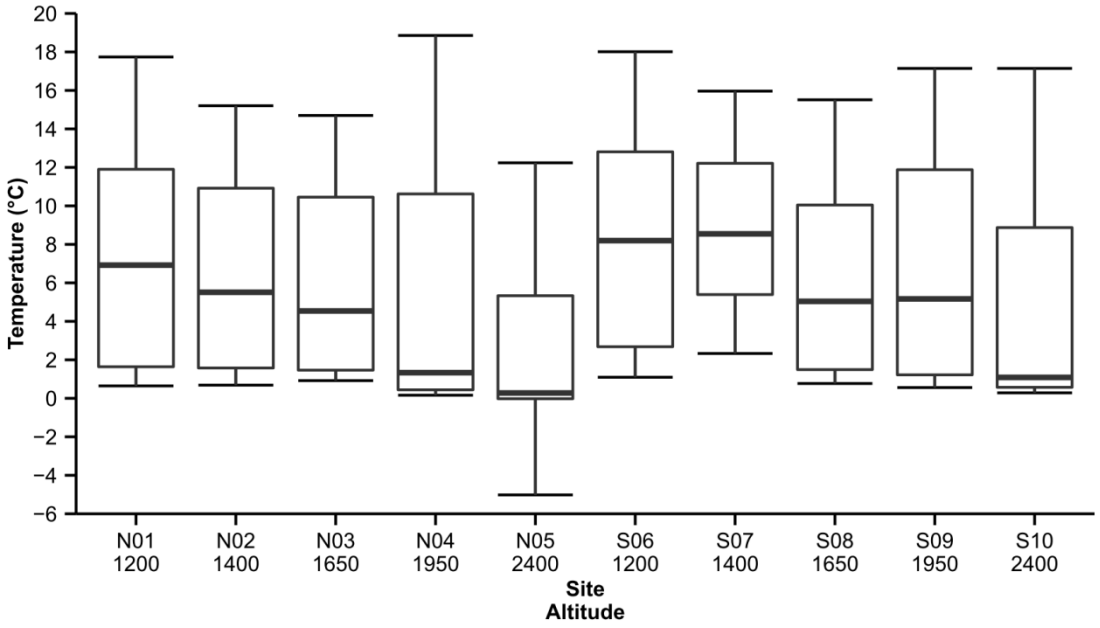


Fig. 4. Site-specific soil temperature, measured between July 2013 and June 2014 (median, 25 and 75 percentile, whiskers maximal 1.5 IQR).

All soils were acidic and the soil pH varied between 4.03 ± 0.03 and 5.76 ± 0.07 (Table 2). The pH values were rather constant with relation to soil depth (0-15 cm). In some soil profiles (N03, N04 and S06), the pH decreased with soil depth. Among north- and south-facing sites soil pH only significantly varied between N02 and S07 and N03 and S08. At all other sites, the pH was not influenced by exposition.

The bulk density varied significantly among control and labeled samples possibly because of the fact that control samples were taken with a core driller and the labeled samples resulted from mesocosms. Overall, the control samples showed higher bulk density values than the labeled samples from the mesocosms. In order to determine SOC stocks, these systematically varying bulk density values posed a risk to the SOC stocks calculation. For that reason, it was decided to calculate mean values per site (control and labeled samples) and calculate the SOC stocks emerging from the bulk density mean values under consideration of error propagation.

Table 2
Soil properties of the climosequence, n=8 (mean (SE))

| Plot | Depth (cm) | Mean annual soil temp. [a] (°C) | Sand [b] (%) | Silt [b] (%) | Clay [b] (%) | Bulk density (g $cm^{-3}$) | Skeleton (%) | pH ($H_20$) [b] | Soil moisture (%) |
|---|---|---|---|---|---|---|---|---|---|
| N01 | 0-5 | 7.3 | 57 | 28 | 16 | 0.55 (0.11) | 0.33 (0.07) | 5.27 (0.02) | 30.8 (4.7) |
| N01 | 5-10 | | 46 | 36 | 18 | 0.85 (0.12) | 0.45 (0.05) | 5.26 (0.09) | 26.0 (4.1) |
| N01 | 10-15 | | 44 | 39 | 17 | 0.81 (0.08) | 0.41 (0.07) | 5.12 (0.09) | 23.4 (5.4) |
| N02 | 0-5 | 6.3 | 41 | 39 | 20 | 0.30 (0.08) | 0.13 (0.03) | 4.54 (0.20) | 42.3 (3.6) |
| N02 | 5-10 | | 38 | 43 | 20 | 0.62 (0.14) | 0.26 (0.06) | 4.32 (0.09) | 42.7 (5.2) |
| N02 | 10-15 | | 39 | 42 | 19 | 0.67 (0.12) | 0.15 (0.07) | 4.58 (0.05) | n.d. |
| N03 | 0-5 | 5.8 | 52 | 26 | 22 | 0.30 (0.11) | 0.27 (0.07) | 4.39 (0.07) | 47.9 (2.7) |
| N03 | 5-10 | | 51 | 37 | 12 | 0.58 (0.12) | 0.32 (0.05) | 4.03 (0.03) | 43.3 (3.7) |
| N03 | 10-15 | | 53 | 32 | 16 | 0.68 (0.14) | 0.25 (0.21) | 4.03 (0.03) | n.d. |
| N04 | 0-5 | 5.0 | 62 | 24 | 14 | 0.64 (0.05) | 0.03 (0.01) | 5.61 (0.07) | 58.0 (3.8) |
| N04 | 5-10 | | 56 | 27 | 17 | 0.85 (0.06) | 0.06 (0.01) | 5.08 (0.05) | 59.9 (2.9) |
| N04 | 10-15 | | 68 | 25 | 7 | 0.85 (0.04) | 0.08 (0.03) | 4.91 (0.15) | 57.0 (5.9) |
| N05 | 0-5 | 2.2 | 61 | 18 | 20 | 0.45 (0.03) | 0.33 (0.05) | 5.10 (0.08) | 52.6 (5.0) |
| N05 | 5-10 | | 55 | 28 | 16 | 0.79 (0.12) | 0.50 (0.07) | 4.95 (0.10) | 47.3 (4.3) |
| N05 | 10-15 | | 53 | 27 | 20 | 0.85 (0.05) | 0.46 (0.06) | 5.05 (0.09) | 52.8 (6.6) |
| S06 | 0-5 | 8.1 | 57 | 29 | 13 | 0.49 (0.03) | 0.15 (0.02) | 5.76 (0.07) | 33.9 (4.2) |
| S06 | 5-10 | | 56 | 31 | 13 | 0.98 (0.04) | 0.33 (0.03) | 5.37 (0.04) | 26.4 (3.4) |
| S06 | 10-15 | | 56 | 31 | 13 | 1.21 (0.09) | 0.36 (0.03) | 5.11 (0.02) | 24.5 (3.6) |
| S07 | 0-5 | 8.7 | 41 | 47 | 12 | 0.49 (0.05) | 0.20 (0.05) | 5.62 (0.04) | 13.3 (1.3) |
| S07 | 5-10 | | 63 | 23 | 14 | 0.82 (0.06) | 0.27 (0.04) | 5.62 (0.05) | 14.7 (1.4) |
| S07 | 10-15 | | 58 | 39 | 3 | 0.87 (0.05) | 0.26 (0.04) | 5.49 (0.05) | n.d. |
| S08 | 0-5 | 6.0 | 62 | 23 | 15 | 0.38 (0.07) | 0.14 (0.04) | 5.46 (0.10) | 34.0 (3.5) |
| S08 | 5-10 | | 42 | 41 | 17 | 0.61 (0.07) | 0.14 (0.02) | 5.61 (0.04) | 30.4 (3.5) |
| S08 | 10-15 | | n.d. | n.d. | n.d. | 0.74 (0.04) | 0.16 (0.03) | n.d. | n.d. |
| S09 | 0-5 | 6.4 | 47 | 29 | 24 | 0.46 (0.04) | 0.04 (0.01) | 5.25 (0.05) | 45.8 (5.1) |
| S09 | 5-10 | | 48 | 29 | 23 | 0.68 (0.03) | 0.05 (0.02) | 5.08 (0.07) | 48.7 (3.5) |
| S09 | 10-15 | | 48 | 30 | 21 | 0.73 (0.03) | 0.05 (0.01) | 5.17 (0.07) | 49.1 (4.0) |
| S10 | 0-5 | 4.5 | 62 | 23 | 15 | 0.46 (0.04) | 0.03 (0.01) | 5.24 (0.05) | 59.1 (7.0) |
| S10 | 5-10 | | 55 | 26 | 20 | 0.76 (0.05) | 0.02 (0.01) | 5.09 (0.08) | 65.0 (7.0) |
| S10 | 10-15 | | 54 | 27 | 19 | 0.91 (0.08) | 0.13 (0.05) | 5.20 (0.04) | 56.0 (3.3) |

[a] Soil temperature was measured and processed by Dr. Kerstin Anschlag and Marta Petrillo; [b] The mineral components and the pH values were measured by Bardelli (2013)

***SOC concentration***

The SOC concentration of the northern gradient (0-5 cm soil depth) increased from the lowest altitude (1200 m a.s.l.), reached the maximum concentration at the altitude of 1650 m a.s.l. (N03) and decreased again toward the high elevated sites (1950 and 2400 m a.s.l.) (Fig. 5, Table 3). The south-facing sites (0-5 cm) were characterized by rather constant SOC concentrations except for the site S08 (1650 m a.s.l.) (Fig. 6). At a depth of 5-10 cm, the SOC concentration of the northern altitudinal gradient followed a similar trend such as the SOC concentration of the 0-5 cm depth did. Nevertheless, the SOC concentration was distinctly (P=0.000, n=40) lower than the concentrations of the 0-5 cm depth (Fig. 5). The 5-10 cm soil depth of the southern altitudinal gradient was characterized by increasing SOC concentration from S06 toward S08 followed by a slight decline of the SOC concentration at the sites S09 and S10. The SOC concentration of the north-facing sites (soil depth of 10-15 cm) peaked at an altitude of 1400 m a.s.l. (N02) and subsequently declined. Meanwhile, the SOC concentration of the south-facing gradient rose continuously with increasing altitude towards the altitude of 1950 m a.s.l. and only slightly declined after that. The SOC concentration did not only vary along the altitudinal gradients, but also among northern and southern expositions. The SOC concentration of the 0-5 cm depth seemed to be higher at north exposed sites than at south-exposed sites. However, the differences between north and south exposed sites were not statistically significant. Considering the sampling depth of 5-10 cm and of 10-15 cm, it was observable that the SOC concentrations of the south-facing slopes were on a level of significance of p=0.1 and thus significantly lower than the SOC concentration at north-facing slopes. Furthermore, all of the soil profiles, except N02, showed declining SOC concentrations with increasing soil depth. Linking the SOC concentration to the climosequence all sampling depths showed a maximum SOM concentration at medium altitude (1400-1950 m a.s.l.) and the SOC concentration of the soil depths 5-10 cm and 10-15 cm were distinctly lower at the southern gradient compared to the northern gradient.

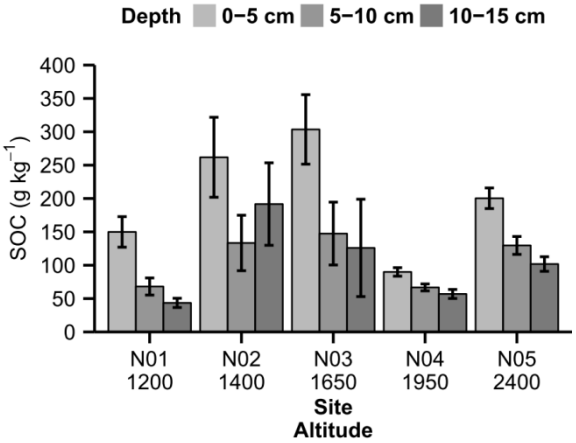


Fig. 5. SOC concentration at northern exposure in 0-5, 5-10 and 10-15 cm soil depth.

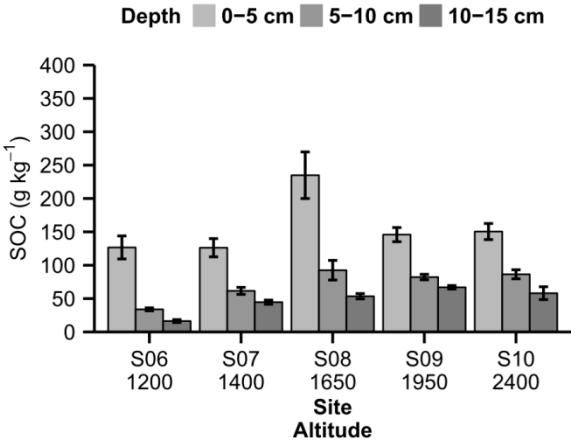


Fig. 6. SOC concentration at southern exposition in 0-5, 5-10 and 10-15 cm soil depth.

***Nitrogen concentration***

The nitrogen concentration in the 0-5 cm horizon of the northern gradient varied between 7.0 ± 0.67 and 9.9 ± 1.51 g $kg^{-1}$ (Fig. 7) and between 5.9 ± 0.62 and 9.3 ± 0.68 g $kg^{-1}$ at the southern sequence (Fig. 8, Table 3). With increasing soil depth the nitrogen concentration declined from the 0-5 cm horizon to the 5-10 cm horizon at both altitudinal gradients ($p<0.05$, n=40). With increasing soil depth (transition 5-10 cm to 10-15 cm) the soil nitrogen concentrations declined again, but only significantly at the south-facing slopes ($p=0.001$, n=40). The 0-5 cm soil depth of the northern altitudinal gradient was characterized by low nitrogen concentrations at an elevation of 1200 m a.s.l. and rather constant nitrogen concentrations at higher elevations. However, the maximum nitrogen concentration was reached at an altitude of 1650 m a.s.l. Nevertheless, the highest site (N05) again revealed distinct nitrogen concentrations. The southern transect showed rising nitrogen concentration with increasing altitude, where the maximum concentration was reached at an elevation of 2400 m a.s.l. However, also the three uppermost sites (1650, 1950 and 2400 m a.s.l.) of the southern transect were characterized by a rather constant nitrogen concentration. The 5-10 cm and 10-15 cm horizon of the northern as well as the southern transect showed rising nitrogen concentrations with increasing altitude. For both soil depths (5-10 and 10-15 cm) and gradients the maximum nitrogen concentration was reached at the highest elevated site (N05 and S10). Exposition-specific differences in nitrogen concentration occurred at the 10-15 cm soil depth, where the northern gradient, on a level of significance of $p=0.1$, showed ($p=0.097$, n=8) elevated nitrogen concentrations compared to the southern altitudinal gradient. Overall, the nitrogen concentration decreased with increasing soil depth. The northern gradient revealed the maximum nitrogen concentration at 1400 m a.s.l. and the southern gradient exhibited increasing nitrogen concentrations with rising altitude (0-5 cm).

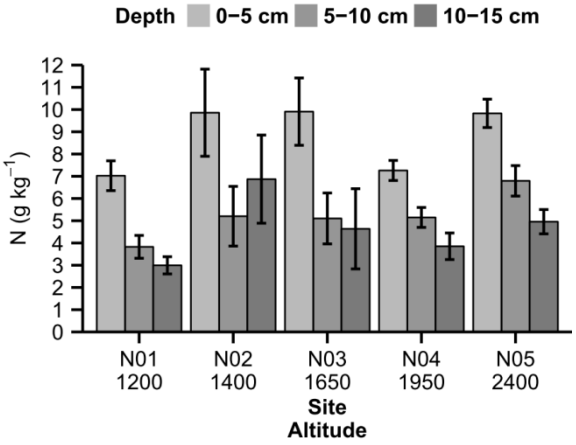


Fig. 7. Nitrogen concentration at the north-facing slopes of the soil depth 0-5, 5-10 and 10-15 cm.

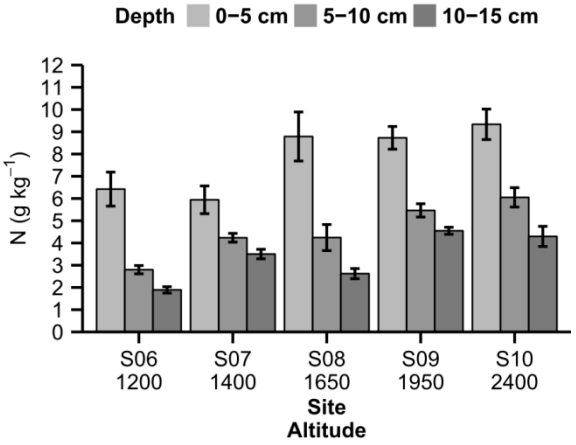


Fig. 8. Nitrogen concentration at the south-facing slopes of the soil depth 0-5, 5-10 and 10-15 cm.

***C/N ratio***

The C/N ratio of both altitudinal sequence and of all investigated soil depths increased towards the altitude of 1650 m a.s.l. and declined at the higher elevated sites (N04 and N05, S09 and S10) (Fig. 9, Fig. 10, Table 3). The C/N ratio of the northern altitudinal gradient varied between 12.4 ± 0.7 and 30 ± 1.6 (0-5 cm depth) and between 16.1 ± 0.41 and 25.8 ± 1.14 at the southern altitudinal sequence. The C/N ratios of the northern gradient seemed to be slightly ($p>0.05$, n=40) higher at the northern

gradient compared to the southern transect. Although, the upper 0-5 cm layer did not show significant differences in C/N ratios between north and south exposed sites, the 5-10 and 10-15 cm layers both revealed distinctly (5-10 cm: p=0.003, n=40; 10-15 cm: p=0.001, n=40) lower C/N ratios at the south-facing slopes compared to the north-facing slopes. Furthermore, the C/N ratios of the northern gradient of most soil depths (0-5 and 10-15 cm) peaked at medium altitude (1650 m a.s.l.). Meanwhile, the C/N ratios of the southern altitudinal sequence showed a delicate increase towards the elevation of 1650 m a.s.l. (S08) for all soil depths followed by a moderate decrease at the sites S09 and S10. Additionally, all sites of the southern gradient showed decreasing C/N ratios with increasing soil depth. The northern altitudinal sequence revealed a rather variable succession of C/N ratios with increasing soil depth. Overall, the C/N ratios of the northern and southern altitudinal gradients peaked at medium elevation (1650 m a.s.l.) of the altitudinal gradients and showed significant lower C/N ratios at the southern gradient at soil depths of 5-10 and 10-15 cm.

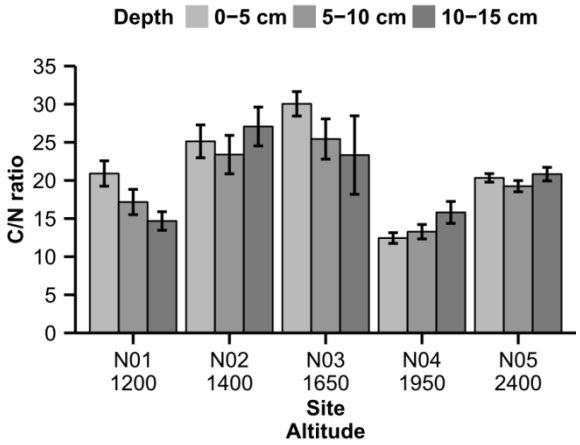


Fig. 9. Site-specific C/N ratios at the northern altitudinal sequence.

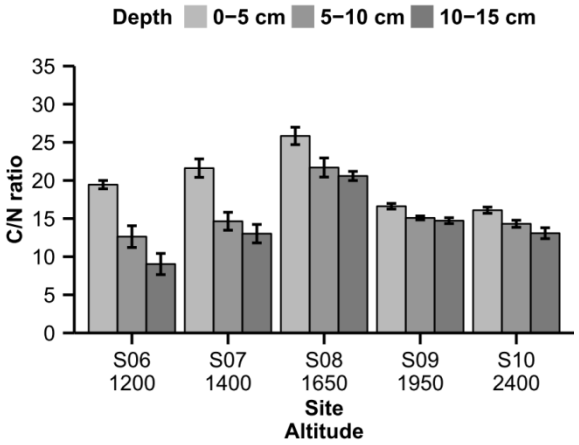


Fig. 10. Site-specific C/N ratios at the southern altitudinal sequence.

***SOC stocks***

The SOC stocks (0-15 cm) ranged between 4.4 ± 0.54 and 9.0 ± 1.20 kg $m^{-2}$ and rose with increasing altitude (Fig. 11, Table 3). The SOC stocks of the north-facing slopes accounted on average for 7.5 ± 0.72 kg $m^{-2}$ and those of the south-facing slopes for 7.0 ± 041 kg $m^{-2}$. However, SOC stocks were not significantly altered by the influence of exposition. Nevertheless, the regimes of SOC stocks differed along the altitudinal gradients. At northern exposures, the SOC stocks reached the maximum magnitude at the elevation of 1400 m a.s.l. and thereafter decreased slightly towards the elevation of 1950 m a.s.l. Meanwhile, the SOC stocks of the southern transect steadily increased from the lowest elevation towards the highest elevation. The SOC stocks of the north-facing slopes were characterized by a strong variability (standard error). For that reason, it was difficult to work out statistically significant differences in SOC stocks between exposition and altitude. Despite this obstacle, it was possible to identify a trend of rising SOC stocks with increasing altitude at the southern gradient. While the northern altitudinal gradient showed a strong increase in SOC stocks at low altitudes followed by stagnating stocks at high altitudes.

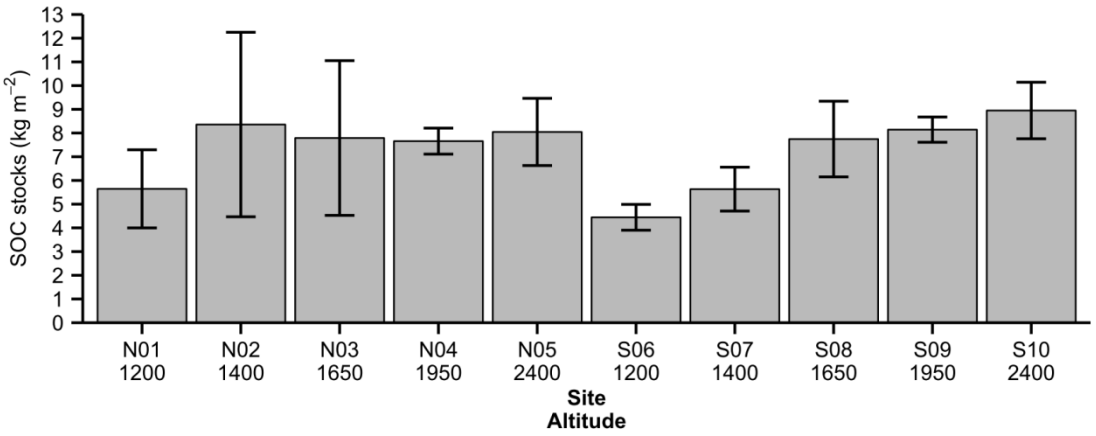


Fig. 11. SOC stocks (0-15 cm) along the northern and southern altitudinal gradient.

## 3.2 Isotopic signature, 13C recovery and priming effect of the bulk soil (0-5 cm)

***Isotopic composition***

The most of the labeled samples significantly differed from the control samples. At the northern gradient, the average $\delta^{13}C$ signal of the control samples accounted for -26.8 ± 0.09 ‰ and the $\delta^{13}C$ signal of the labeled samples was on average 0.5 ± 0.19 ‰ less negative than the control samples (Fig. 12). The control samples of the southern gradient were characterized by mean $\delta^{13}C$ values of -27.0 ± 0.19 ‰ and the labeled samples were on average 1.1 ± 0.16 ‰ less negative than the control samples (Fig. 13). Along the northern elevation sequence, the moderately elevated control sites showed more negative $\delta^{13}C$ values than the highly elevated sites. Meanwhile, the labeled plots of the same sites exhibited a continuous increase of the $\delta^{13}C$ values towards less negative values at higher altitudes (Fig. 12). Two of five (N04 and N05) labeled plots of the northern gradient were characterized by significantly ($p<0.05$, $n=4$) enriched $\delta^{13}C$ signals compared to the control plots. At the southern altitudinal gradient the $\delta^{13}C$ values of the control plots declined at moderate altitude toward more negative $\delta^{13}C$ levels, reached the minimum at 1650 m a.s.l. and rose again toward less negative $\delta^{13}C$ values at higher altitudes (Fig. 13). The $\delta^{13}C$ values of the labeled plots of the southern gradient continuously decreased towards more negative $\delta^{13}C$ levels with increasing altitude. Thus, the difference in the $\delta^{13}C$ signals between control and labeled plots decreasing steadily with increasing altitude. Statistics confirmed this trend as the moderately elevated sites (S06, S07, S08 and S09) showed distinct differences ($p<0.05$, $n=4$) of $\delta^{13}C$ values between control and labeled plots while the sites S09 and S10 manifested only small differences between the $\delta^{13}C$ signals. Additionally, it is to mention that all labeled plots except N02 revealed less negative $\delta^{13}C$ signals than the control plots of the same site. This was expected due to the addition of highly enriched $\delta^{13}C$ substrate to soil samples with natural isotopic abundance. The $^{13}C$ recovery of a sampling site is calculated by the differences among the $\delta^{13}C$ values of control and labeled samples. Therefore higher differences between control and labeled samples cause by tendency larger $^{13}C$ recoveries. Hence, sites with significant differences between control and labeled plots also showed larger substrate recovery at the same sites. Exposure-specific differences in $\delta^{13}C$ signals between the northern and southern gradient did not occur.

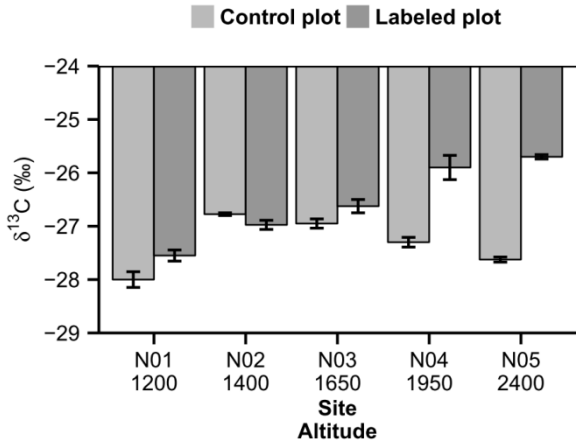


Fig. 12. $\delta^{13}C$ signal of the bulk soil (0-5 cm) at the northern elevation sequence.

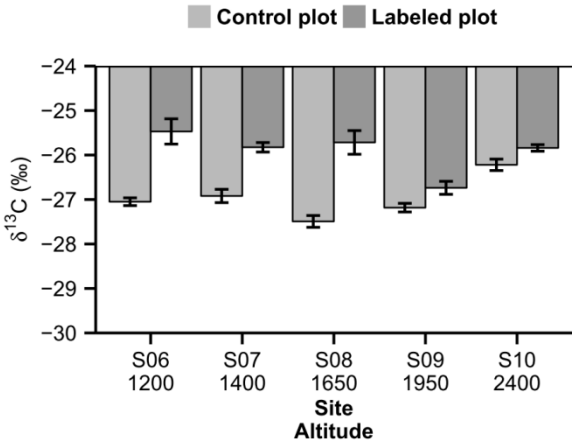


Fig. 13. $\delta^{13}C$ signal of the bulk soil (0-5 cm) at the southern elevation sequence.

***$^{13}C$ recovery***

The $^{13}C$ recovery calculated according to the formula (3) and with the use of 43.3 ‰ for the term $\delta^{13}C_{substrate}$ led to site-specific recoveries as shown in figure 14. At the northern altitudinal gradient the $^{13}C$ recovery varied between 0 ± 0.24 % (N02) and 2.3 ± 0.11 % (N05) while the $^{13}C$ recoveries of the southern gradient ranged from 0.5 ± 0.27 % (S10) to 2.5 ± 0.34 % (S08) (Table 3). On average, the northern gradient revealed substrate recoveries of 0.8 ± 0.21 % and the southern transect 1.5 ± 0.19 %. For all statistical evaluations the negative $^{13}C$ recoveries of the site N02 were set to zero, since negative substrate recoveries are not possible. Under the assumption that natural spruce litter was decomposed similarly to the applied substrate ($^{13}C$ labeled Norway spruce needles) one can assume that the same amount of the naturally deposited spruce litter is recovered after one year. Nevertheless, one should not forget that the experiment was conducted with milled needles and not with fresh needles. However, all $^{13}C$ that was not recovered after an one year was either mineralized by microorganisms to $CO_2$ or lost by DOC leaching (Kammer and Hagedorn, 2011). Along the northern altitudinal gradient a trend of increasing substrate recoveries with increasing altitude was observed. The $^{13}C$ recovery rose significantly between the lowest elevated site (N01) and the highest elevated site (N05). The south exposed altitudinal gradient exhibited rather high $^{13}C$ recoveries at the low- and mid-elevated sites (S06, S07 and S08) followed by a decrease in $^{13}C$ recoveries at the higher located sites (S09 and S10). According to figure 14, the $^{13}C$ recovery of the southern gradient dropped significantly between the elevation of 1650 and 1950 m a.s.l. The comparison of all substrate recoveries of both gradients revealed significantly lower $^{13}C$ recoveries at the northern altitudinal gradient ($p=0.038$, $n=20$). Overall, the $^{13}C$ recoveries of all sites were rather heterogeneous and the identification of trends along the gradients was difficult.

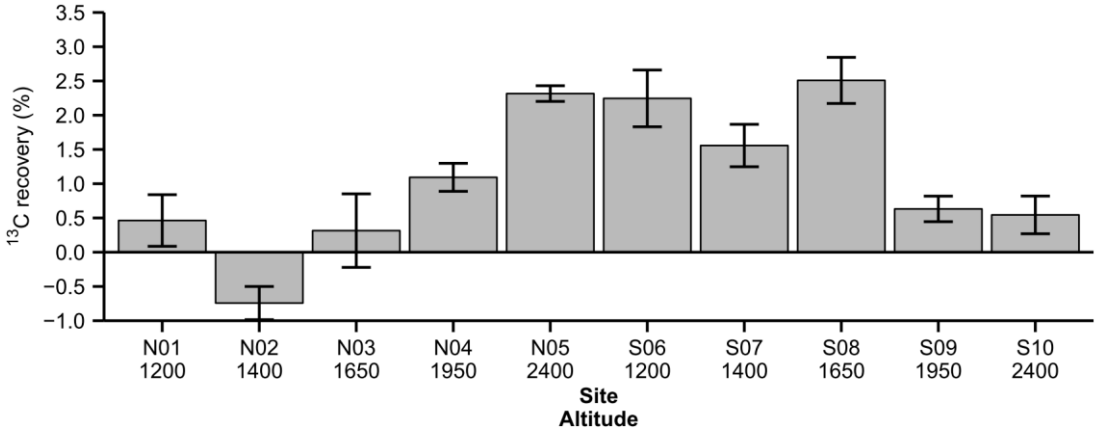


Fig. 14. Site-specific $^{13}$C recoveries of the bulk soil (0-5 cm).

Another option to calculate the $^{13}$C recovery emerges from the assumption that the applied substrate will be diluted by the natural $^{13}$C signal of the soil. The mixing of a little amount of a $^{13}$C labeled substrate with a larger amount of natural soil will cause a reduction of the $^{13}$C signal of the resulting labeled soil sample. To what extent the $^{13}$C label of the substrate will be diluted depends on the carbon amount of the substrate and of the soil sample as well as on the magnitude of the $^{13}$C label of the substrate and the initial $\delta^{13}$C signature of the natural soil. Using the diluted $\delta^{13}$C signal of the mixed soil sample with the substrate for the term $\delta^{13}C_{substrate}$ in formula (3) led to distinctly higher $^{13}$C recoveries for all analyzed sites (Fig. 15). On average, the north-facing altitudinal gradient showed a $^{13}$C recovery of 25.1 ± 6.99 % while the south-facing gradient revealed a mean $^{13}$C recovery of 34.7 ± 4.77 %. The northern altitudinal gradient was characterized by low $^{13}$C recoveries at moderate altitudes (N01, N02, N03, and N04). Towards the higher elevated site the $^{13}$C recovery rose significantly ($p=0.029$, $n=4$). The southern altitudinal transect showed rather high substrate recoveries at the moderately elevated sites (S06, S07 and S08) while the more elevated sites (S09 and S10) showed reduced substrate recoveries. Overall, no significant exposition-specific substrate recoveries were observable ($p>0.05$, $n=20$).

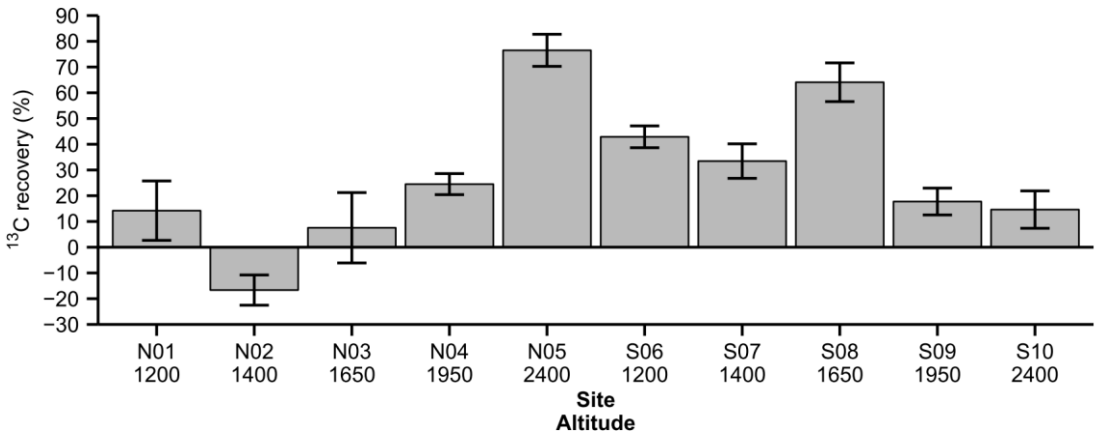


Fig. 15. Site-specific $^{13}$C recoveries (diluted substrate) of the bulk soil (0-5 cm).

***Priming effect***

The priming effect (PE) was positive at the northern gradient with the exception of site N05 and negative at the southern gradient with the exception of site N07 (Fig. 16). On average, the northern altitudinal gradient showed PE value of 68.2 ± 34.9 g $kg^{-1}$ and the southern elevation sequence -57.6 ± 16.8 g $kg^{-1}$.

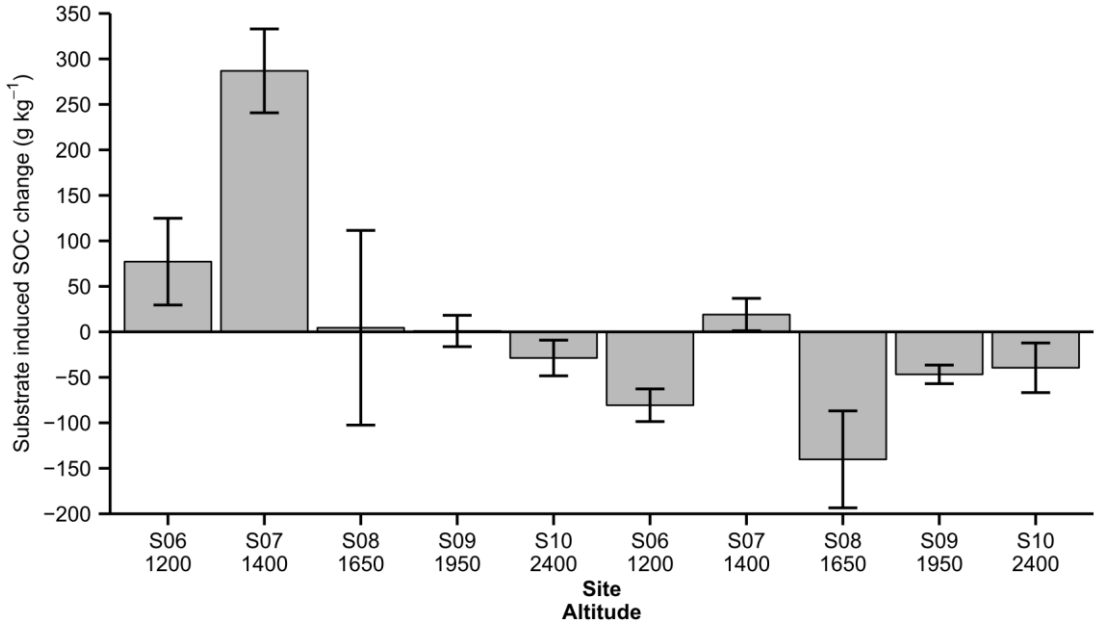


Fig. 16. Site-specific priming effect in the upper 0-5 cm of the bulk soil due to substrate amendment.

Table 3
Chemical and physical properties of the fine earth (<2 mm) of the investigated soils, n=[a,b] ,(mean (SE))

| Plot | Depth (cm) | SOC[a] (g $kg^{-1}$) | N tot[a] (g $kg^{-1}$) | C/N ratio[a] | SOC-stocks[a] (kg $m^{-2}$) | $\delta^{13}$C control[b] (‰) | $\delta^{13}$C label[b] (‰) | $^{13}$C recovery[b] (%) | $^{13}$C recovery (diluted substrate)[b] (%) |
|---|---|---|---|---|---|---|---|---|---|
| N01 | 0-5 | 149.9 (22.9) | 7.02 (0.67) | 20.9 (1.7) | 5.65 (1.65) | -29.86 (0.62) | -27.06 (0.20) | 0.46 (0.38) | 14.20 (11.54) |
| N01 | 5-10 | 68.1 (12.8) | 3.83 (0.51) | 17.2 (1.7) | | -29.41 (0.19) | -28.71 (0.23) | | |
| N01 | 10-15 | 43.6 (6.9) | 3.00 (0.39) | 14.7 (1.2) | | -28.24 (0.28) | -28.72 (0.25) | | |
| N02 | 0-5 | 261.8 (59.9) | 9.86 (1.96) | 25.1 (2.2) | 5.65 (3.89) | -29.86 (0.11) | -26.98 (0.08) | -0.74 (0.24) | -16.66 (5.87) |
| N02 | 5-10 | 133.4 (41.6) | 5.20 (1.34) | 23.4 (2.5) | | -27.46 (0.30) | -27.62 (0.30) | | |
| N02 | 10-15 | 191.7 (61.8) | 6.87 (1.98) | 27.1 (2.5) | | -28.44 (0.21) | -28.43 (0.23) | | |
| N03 | 0-5 | 303.6 (52.1) | 9.91 (1.51) | 30 (1.6) | 7.79 (3.26) | -28.87 (0.12) | -26.40 (0.22) | 0.32 (0.54) | 7.55 (13.67) |
| N03 | 5-10 | 147.5 (47.1) | 5.10 (1.14) | 25.4 (2.6) | | -27.93 (0.30) | -26.51 (0.50) | | |
| N03 | 10-15 | 126.0 (73.0) | 4.64 (1.80) | 23.3 (5.1) | | -27.90 (0.31) | -27.03 (0.64) | | |
| N04 | 0-5 | 90.0 (6.3) | 7.26 (0.45) | 12.4 (0.7) | 7.66 (0.55) | -28.08 (0.36) | -25.87 (0.19) | 1.09 (0.20 | 24.51 (4.09) |
| N04 | 5-10 | 66.8 (5.2) | 5.15 (0.45) | 13.3 (0.9) | | -30.06 (0.40) | -29.08 (0.12) | | |
| N04 | 10-15 | 56.9 (6.7) | 3.85 (0.60) | 15.8 (1.4) | | -29.48 (0.20) | -28.88 (0.12) | | |
| N05 | 0-5 | 200.4 (15.4) | 9.83 (0.64) | 20.3 (0.6) | 8.05 (1.42) | -28.76 (0.39) | -25.35 (0.06) | 2.32 (0.11) | 76.50 (6.23) |
| N05 | 5-10 | 129.7 (13.4) | 6.79 (0.68) | 19.2 (0.7) | | -28.36 (0.26) | -28.06 (0.51) | | |
| N05 | 10-15 | 101.8 (10.9) | 4.96 (0.55) | 20.8 (0.9) | | -29.47 (0.51) | -28.23 (0.07) | | |
| S06 | 0-5 | 126.7 (17.2) | 6.42 (0.76) | 19.4 (0.5) | 4.45 (0.54) | -28.55 (0.16) | -25.47 (0.28) | 2.25 (0.41) | 42.88 (4.24) |
| S06 | 5-10 | 33.9 (2.2) | 2.80 (0.19) | 12.6 (1.4) | | -28.28 (0.18) | -28.53 (0.05) | | |
| S06 | 10-15 | 16.3 (2.2) | 1.89 (0.14) | 9.0 (1.4) | | -28.79 (0.08) | -28.46 (0.08) | | |
| S07 | 0-5 | 126.3 (13.7) | 5.94 (0.62) | 21.6 (1.2) | 5.63 (0.92) | -28.54 (0.14) | -25.83 (0.11) | 1.56 (0.31) | 33.46 (6.70) |
| S07 | 5-10 | 61.6 (5.3) | 4.24 (0.20) | 14.6 (1.2) | | -28.61 (0.28) | -28.64 (0.62) | | |
| S07 | 10-15 | 44.7 (3.1) | 3.50 (0.21) | 13.0 (1.2) | | -29.33 (0.35) | -28.51 (0.14) | | |
| S08 | 0-5 | 234.9 (34.9) | 8.79 (1.10) | 25.8 (1.1) | 7.75 (1.60) | n.d. | -25.72 (0.27) | 2.51 (0.34) | 64.09 (7.52) |
| S08 | 5-10 | 92.5 (14.7) | 4.24 (0.59) | 21.7 (1.3) | | -29.09 (0.00) | -27.39 (0.15) | | |
| S08 | 10-15 | 53.5 (4.0) | 2.62 (0.23) | 20.6 (0.6) | | -29.30 (0.06) | -28.68 (0.12) | | |
| S09 | 0-5 | 145.9 (10.6) | 8.73 (0.51) | 16.6 (0.4) | 8.14 (0.53) | -26.23 (0.66) | -26.74 (0.15) | 0.63 (0.19) | 17.75 (5.21) |
| S09 | 5-10 | 82.2 (4.1) | 5.46 (0.30) | 15.1 (0.3) | | -29.11 (0.40) | -29.42 (0.20) | | |
| S09 | 10-15 | 66.9 (2.6) | 4.55 (0.16) | 14.7 (0.4) | | -27.06 (0.48) | -28.80 (0.07) | | |
| S10 | 0-5 | 150.5 (12.1) | 9.34 (0.68) | 16.1 (0.4) | 8.95 (1.19) | -28.75 (0.08) | -25.84 (0.07) | 0.54 (0.28) | 14.61 (7.26) |
| S10 | 5-10 | 86.5 (6.8) | 6.05 (0.44) | 14.3 (0.5) | | -28.55 (0.16) | -28.04 (0.17) | | |
| S10 | 10-15 | 58.1 (9.6) | 4.30 (0.45) | 13.1 (0.7) | | -28.35 (0.17) | -25.88 (0.77) | | |

[a] n=8, [b] n=4

## 3.3 Density fractionation (0-5 cm)

***Mass and carbon recovery***

The mass balance of the density fractionation showed mean mass recovery after density fractionation of 95.4 ± 0.3 %. On the one hand, material losses occurred due to ultrasonic treatment of the soil samples and on the other because of imperfect settlement of the fractions after centrifuging the samples. The losses during the ultrasonic treatment did not result because of the ultrasonic treatment itself but rather due to the difficulty to remove all soil material after the treatment from the ultrasonic device. The carbon recovery accounted for 91.4 ± 1.1% after density fractionation. Carbon losses during the density fractionation occurred either because of material losses or due to carbon mobilization into the SPT solution and into the applied water, which was used to remove the SPT solution from the samples (Singh et al., 2014).

Significant amounts of soil mass were found in the HF (P=0.000, n=160) of the upper 5 cm soil layer (Fig. 17, Table 4). At the north-facing slopes, the contribution of the LF to the total sample mass was on average 31.9 ± 5.0 % and 21.0 ± 2.9 % at the south-facing sites respectively. The HF of the northern gradient contained on average 68.1 ± 5.0 % and the south-facing sites 79.0 ± 2.9 % of the total sample mass. Along both gradients the LF was characterized by maximum mass percentages at an elevation of 1650 m a.s.l. (N03 and S08). However, the LF of the southern gradient seemed to contain less soil mass than the LF of the northern gradient, which cannot be statistically confirmed (P=0.386, n=20). Nevertheless, the mass percentage of the LF peaked at northern exposition at the site N03 and decreased with higher altitudes. In addition to this, the influence of exposition was investigated and it seemed that the south-facing sites showed lower LF mass percentages than the north exposed sites. Unfortunately, this observation cannot be statistically confirmed either. Above all, along both elevation transects the soil mass percentages of the LF increased at low-elevated sites peaked at an altitude of 1650 m a.s.l. and declined again with higher altitude. Furthermore, there appears to be only a small influence of exposition on the LF mass percentage. The mass percentages of the HF behaved inversely to the soil mass percentages of the LF.

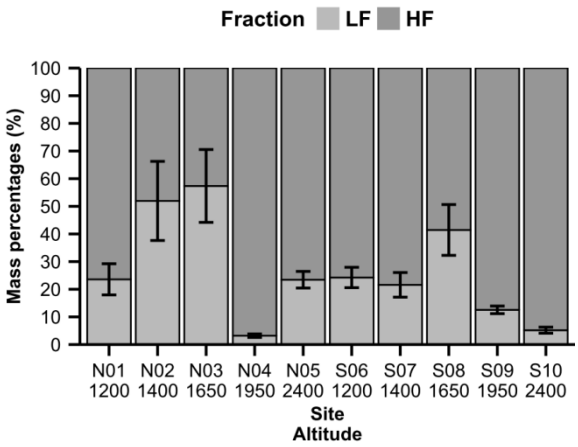


Fig. 17. Mass percentage of the LF and HF per site (0-5 cm).

***Fraction dependent SOC concentration***

The SOC concentration in the LF at north-facing slopes and south-facing slopes ranged from 418.5 to 462.8 g $kg^{-1}$ and 401.0 to 446.0 g $kg^{-1}$ respectively (Fig. 18, Fig. 19, Table 4). In the HF, the SOC concentration of the northern and southern exposition varied between 61.9 and 181.3 g $kg^{-1}$ and 39.2 and 139.0 g $kg^{-1}$ respectively. Maximum SOC concentration of the LF occurred for both altitudinal gradient at the elevation of 1650 m a.s.l. (N03 and S08). Overall, the SOC concentration of the LF of both gradients showed rather constant values and did not change significantly. Furthermore, the SOC concentration of the LF did not vary distinctly between the two altitudinal gradients. The SOC concentration of the HF showed different trends at the two gradients. At northern expositions the maximum SOC concentration of the HF was reached at 1650 m a.s.l. (N03), however no significant increase in the SOC concentration was observed. Thereafter, the SOC concentration decreased with increasing altitude. Meanwhile, the HF of the southern gradient showed rising SOC concentration with increasing altitude. Hence, highest SOC concentration of the southern gradient was recognized at the highest elevated site (S10). The regime of SOC concentration of the HF differed between the two gradients but no significant differences were found in the magnitude of the values.

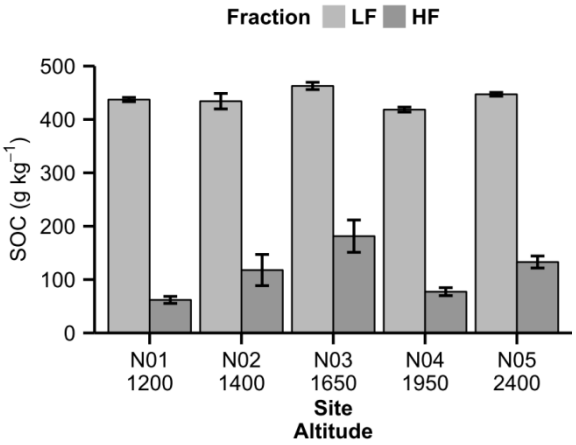


Fig. 18. SOC concentration of the LF and HF at the northern altitudinal gradient (0-5 cm).

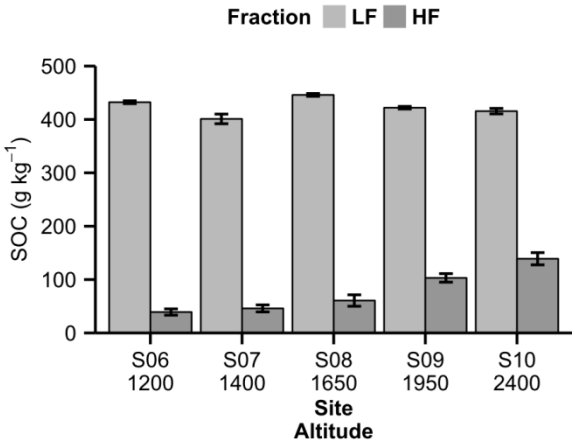


Fig. 19. SOC concentration of the LF and HF at the southern altitudinal gradient (0-5 cm).

***Fraction dependent nitrogen concentration***

The mean nitrogen concentration in the LF of the northern altitudinal gradient accounted for 16.3 ± 1.1 g $kg^{-1}$ while the southern elevation gradient exhibited mean nitrogen concentration in the LF of 16.7 ± 0.5 g $kg^{-1}$. The HF was characterized at the northern gradient by a mean nitrogen concentration of 6.4 ± 0.7 g $kg^{-1}$ and at the southern gradient by a mean nitrogen concentration of 4.8 ± 0.6 g $kg^{-1}$. The nitrogen concentration of the LF seemed to decrease with increasing altitude. Nevertheless, a shift occurred between the sites N03 and N04, where the nitrogen concentration of the LF jumped to distinctly higher values of concentration (Fig. 20, Fig. 21). Therefore, both gradients revealed a significant (northern gradient: p=0.000, n=8; southern gradient: p=0.000, n=8) increase of the nitrogen concentration between the sites N03 and N04 and between S08 and S09 respectively. Thereafter, both gradients again showed declining nitrogen concentration with increasing altitude at the grass-dominated sites. Meanwhile, the HF of the northern gradient reached its maximum nitrogen concentration at medium altitude (1650 m a.s.l.) and the southern gradient was characterized by a significant increase in nitrogen concentration with increasing altitude. The HF of

the northern gradient showed significantly (p=0.018, n=40) higher nitrogen concentration compared to the southern gradient, while the nitrogen concentration of the LF was in the same range for both gradients (p=0.167, n=40). Furthermore, both altitudinal gradients exhibited significantly (both gradients: p=0.000, n=40) lower nitrogen concentration in the HF compared to the LF.

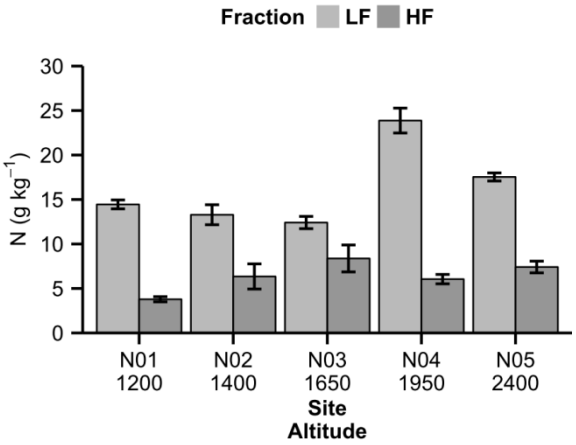


Fig. 20. Total nitrogen of the LF and HF at the northern altitudinal gradient.

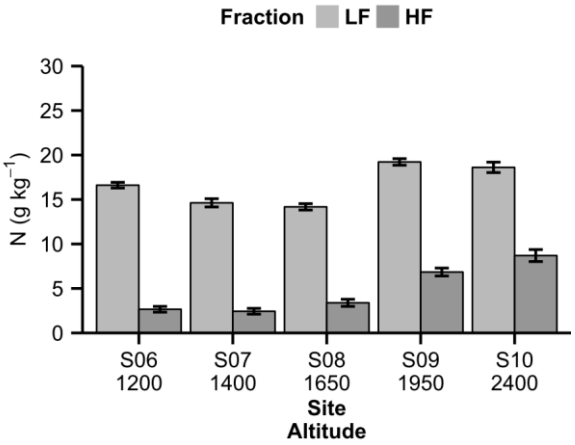


Fig. 21. Total nitrogen of the LF and HF at the southern gradient.

***Density fraction-specific carbon and nitrogen distribution***

In order to investigate carbon storage potential of the soil fractions it is of interest how OC is distributed in different soil fractions. Along the northern altitudinal gradient on average 55.4 ± 4.4 % of the SOC was recovered in the LF, while the HF showed mean values of OC recovery of 44.6 ± 4.4 %. The LF of the southern gradient was characterized by mean values of OC recovery of 53.6 ± 4.5 %, while the HF showed mean OC recovery of 46.4 ± 4.5 %. The LF of both gradients revealed large OC recoveries at low elevated sites while at high altitudes the OC recovery dominated in the HF (Fig. 22). A maximum OC recovery in the LF of the northern and southern gradient was found at an altitude of 1650 m a.s.l. (N03 and S08). At the altitude of 1950 m a.s.l. and 2400 m a.s.l. mainly the OC of the HF contributed to total OC. The fraction-dependent carbon distribution was exposure-dependent.

Nitrogen was similarly distributed along the altitudinal gradients as the OC, although the magnitudes varied between the OC and nitrogen distributions (Fig. 23, Table 4). The LF of the northern gradient showed mean nitrogen amounts of 46.7 ± 4.6 %, while in the HF of the northern gradient on average 53.3 ± 4.6 % of the nitrogen was recovered. Along the southern gradient on average 45.8 ± 4.3 % of the nitrogen was recovered in the LF, while the HF exhibited mean values of nitrogen recovery of 54.2 ± 4.3 %. The nitrogen distribution of both density fractions was not affected by exposure-specific influences (p=0.815, n=40).

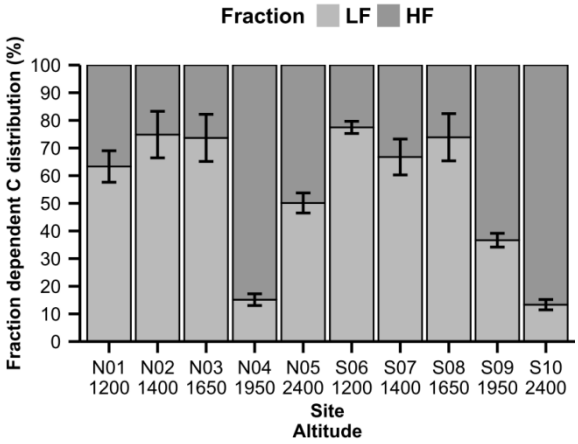


Fig. 22. Site-specific carbon distribution in the LF and HF (0-5 cm).

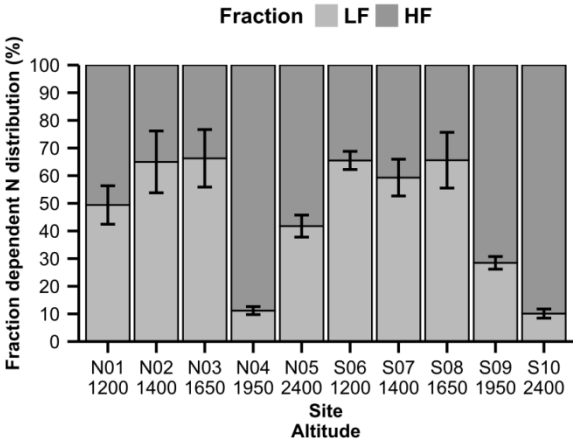


Fig. 23. Site-specific nitrogen distribution in the LF and HF (0-5 cm)

***Fraction-specific C/N ratio***

The average C/N ratio of the LF at the north-facing gradient amounted to 29.4 ± 2.0, while the mean C/N ratio of the LF of the south-facing sequence accounted for 26.0 ± 0.9. In contrast to this, the C/N ratio of the HF of both gradients was distinctly (northern and southern gradient: p=0.000, n=40) lower than the C/N ratio of the LF. The average C/N ratio of the HF of the northern gradient was 17.7 ± 1.1 and 16.3 ± 0.5 at the southern gradient. The differences between the C/N ratios of the LF and HF accounted at the northern gradient on average for 11.74 ± 1.03 and at the southern gradient for 9.70 ± 0.56. Hence, the differences between the C/N ratios of the LF and HF were more pronounced at the northern gradient.

The C/N ratios of both fractions of the northern transect showed slightly higher values than the south-facing sites (Fig. 24, Fig. 25). Nevertheless, the differences were not statistically significant (LF: p=0.056, n=20; HF: p=0.140, n=20). Along both gradients the C/N ration of the LF dropped at the transition from 1650 m a.s.l. to 1950 m a.s.l. (northern gradient: p=0.000, n=8; southern gradient: p=0.004, n=8). The LF of the northern and southern gradient was characterized by rising nitrogen concentration with increasing altitude until the nitrogen concentration dropped at the higher elevated sites (Fig. 24, Fig. 25). The HF of the northern gradient also exhibited a drop in the C/N ratio between the sites N03 and N04 (p=0.000, n=8), while the HF of the southern gradient was characterized by declining C/N ratios starting from the elevation of 1400 m a.s.l. towards the highest elevated site (S10, 2400 m a.s.l.).

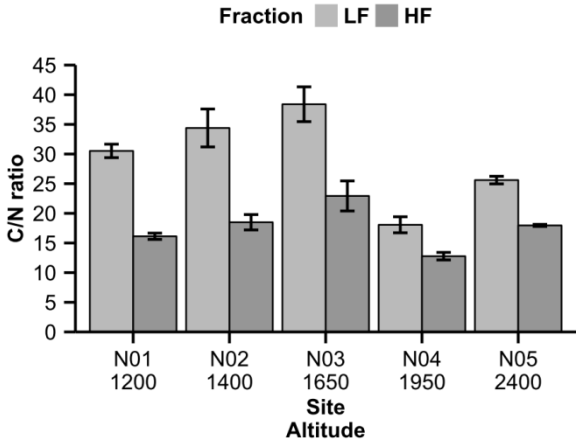


Fig. 24. Fraction-specific C/N ratio at the northern altitudinal gradient

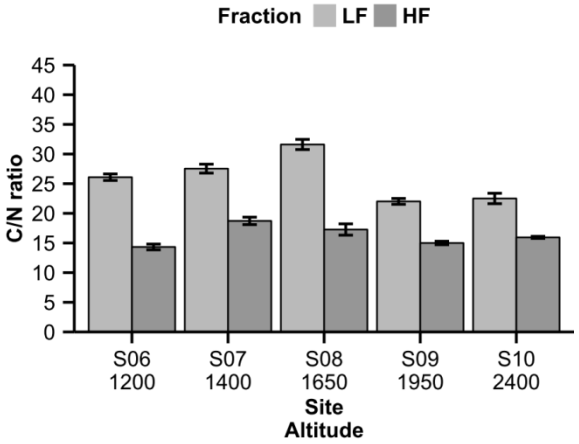


Fig. 25. Fraction-specific C/N ratio at the southern altitudinal gradient

***Fraction dependent isotopic signature***

In the 0-5 cm layer the $\delta^{13}C$ signal of the LF was distinctly more negative than the $\delta^{13}C$ signal of the HF (control: p=0.00, n=40 and label: p=0.000, n=40). The LF of the control plots of the northern gradient showed on average a $\delta^{13}C$ signal of -27.33 ± 0.11 ‰ (Fig. 26) and the LF of the southern gradient a mean $\delta^{13}C$ value of -27.53 ± 0.09 ‰ (Fig. 27). The differences between $\delta^{13}C$ values of the control samples did not differ significantly between the two expositions. At the same time, the HF of the control plots of the northern gradient revealed a mean $\delta^{13}C$ value of -26.39 ± 0.10 ‰ (Fig. 28) and the south-facing sites a mean $\delta^{13}C$ value of -26.27 ± 0.07 ‰ (Fig. 29). Therefore, the $\delta^{13}C$ signal of the southern gradient was slightly less negative than the $\delta^{13}C$ signature of the northern gradient, although the differences were not statistically significant. Differences in the natural isotopic signature (control soil) between the two density fractions showed the following pattern: the northern gradient showed differences in the $\delta^{13}C$ signal of 0.93 ± 0.11 ‰ and the southern gradient of 1.27 ± 0.06 ‰. Hence, the southern gradient revealed significantly larger (p=0.018, n=20) isotopic differences between the LF and HF than the northern gradient. The regime of the $\delta^{13}C$ values along the northern gradient (control soil) was characterized by the maximum (the least negative) $\delta^{13}C$ signal at the site N02 (Fig. 26). Meanwhile, the southern gradient showed decreasing $\delta^{13}C$ values in the LF with increasing altitude (Fig. 27). The $\delta^{13}C$ signal of the HF (control soil) remained rather constant at both altitudinal gradients (Fig. 28, Fig 29).

The labeled plots of the northern gradient exhibited mean $\delta^{13}C$ values of -26.55 ± 0.17 ‰ (LF) and -25.87 ± 0.15 ‰ (HF), while the southern gradient showed on mean $\delta^{13}C$ signals of -26.19 ± 0.16 ‰ (LF) and -25.45 ± 0.16 ‰ (HF). The comparison of the $\delta^{13}C$ values of the control and labeled samples of the LF per site revealed a distinct ($P<0.05$) enrichment of the $\delta^{13}C$ signal in the labeled samples for most of the sites (N04 -N05 and S06 -S10). In the HF, only the sites N05, S06 and S07 showed a significant enrichment in $^{13}C$ of the labeled samples. The grassland sites of the northern gradient (N04 and N05 of the LF) were characterized by the largest differences between control and labeled plots (Fig. 25), while the southern altitudinal sequence revealed the most distinct differences among control and labeled plots at the forest sites (S06, S07 and S08 of the LF) (Fig. 26). A similar pattern can be observed for the HF of both gradients (Fig. 28, Fig. 29). Surprising differences between control and labeled plots can be found at the site N02, where both density fractions were characterized by

more negative $\delta^{13}C$ values in the labeled plots than in the control plots. Nevertheless, the differences were small and likely caused by measurement inaccuracy.

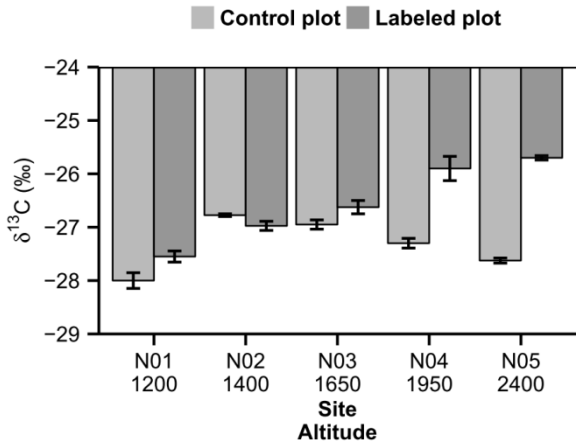


Fig. 26. Site-specific $\delta^{13}C$ signature of the control and labeled plots of the LF at the northern altitudinal gradient.

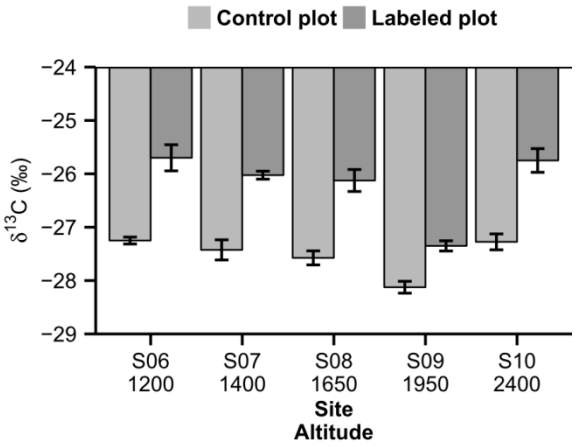


Fig. 27. Site-specific $\delta^{13}C$ signature of the control and labeled plots of the LF at the southern altitudinal gradient.

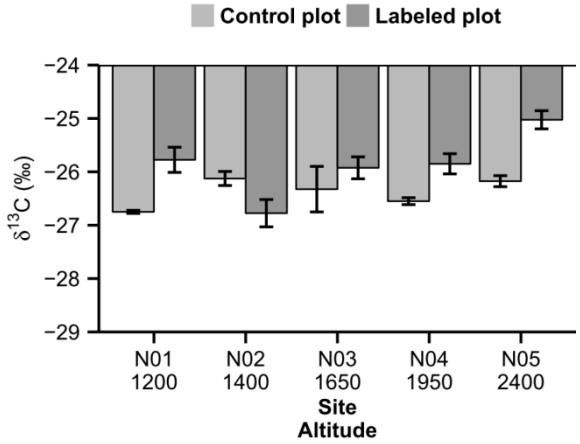


Fig. 28. Site-specific $\delta^{13}C$ signature of the control and labeled plots of the HF at the northern altitudinal gradient

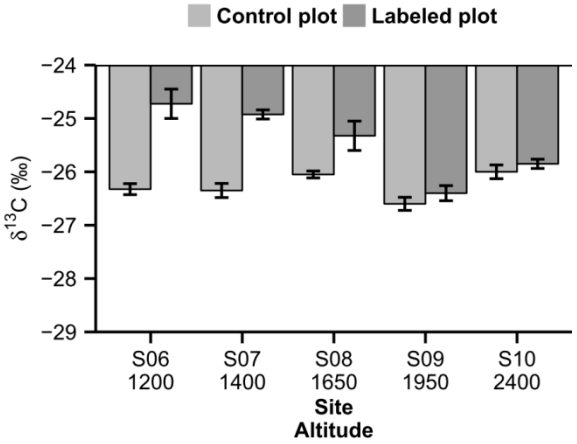


Fig. 29. Site-specific $\delta^{13}C$ signature of the control and labeled plots of the HF at the southern altitudinal gradient

The mean $\delta^{15}N$ composition of the northern gradient accounted for -0.76 ± 0.70 ‰ (LF) and 1.36 ± 0.60 ‰ (HF). The southern gradient was characterized by mean $\delta^{15}N$ signatures of -1.35 ± 0.41 ‰ (LF) and 0.55 ± 0.45 ‰ (HF). According to this observation, the northern gradient exhibited higher mean $\delta^{15}N$ values than the southern gradient, although the mean values did not differ significantly (LF: p=0.829, n=20; HF: p=0.337, n=20) (Fig. 30, Fig. 31). However, along both gradients the HF revealed distinctly less negative $\delta^{15}N$ values compared to the LF (northern gradient: p=0.004, n=20; southern gradient: p=0.006, n=20) (Fig. 30, Fig, 31). Furthermore, the mean differences in isotopic signatures between the LF and HF amounted to 2.10 ± 0.28 ‰ at the northern gradient and to 1.90 ± 0.12 ‰ at the southern gradient. Hence, the isotopic differences in $\delta^{15}N$ values between the LF and HF did not show distinct differences between both gradients (p=0.513, n=20).

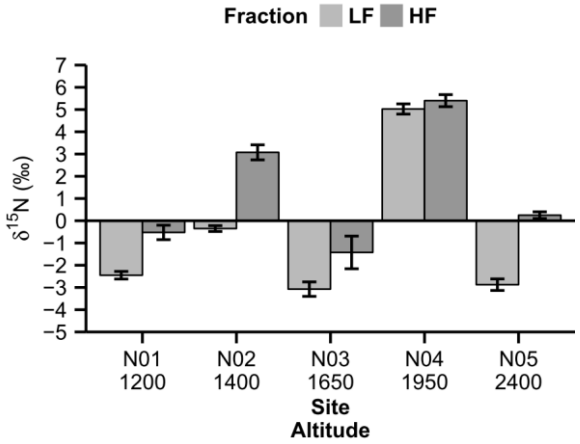


Fig. 30. Fraction-dependent $\delta^{15}N$ signature of the northern gradient (0-5) cm

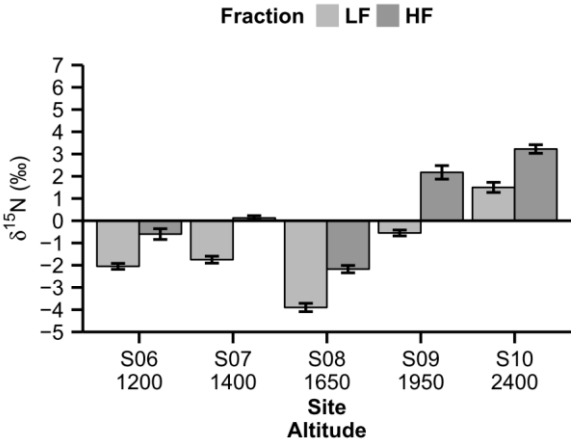


Fig. 31. Fraction-dependent $\delta^{15}N$ signature of the southern gradient (0-5) cm

***Fraction-specific $^{13}C$ recovery***

The $^{13}C$ recovery (remaining $^{13}C$ from the initial Norway spruce needle powder) after one year of field stay in the LF at northern exposition accounted on average for 1.1 ± 0.26 % and at southern exposition for 1.9 ± 0.17 % (Fig. 32, Fig. 33, Table 4). In the HF at northern exposition on average 0.7 ± 0.04 % and at southern exposition 1.2 ± 0.23 % of the initial applied $^{13}C$ was recovered. The $^{13}C$ recovery in the LF at north-facing slopes varied between 0 and 2.3 ± 0.12 % and at south-facing slopes between 1.1 ± 0.16 % and 2.2 ± 0.38 %. The HF of the northern gradient was characterized by $^{13}C$ recoveries between 0 and 1.7 ± 0.31 % and at southern exposure between 0.21 ± 0.29 % and 2.3 ± 0.47 %. The northern sites N01, N02 and N03 showed significantly ($p<0.05$, n=4) lower $^{13}C$ recoveries than the south-facing sites of the same elevation. By contrast, the HF was not affected by exposition-specific $^{13}C$ recoveries. The LF of the northern altitudinal gradient was characterized by increasing $^{13}C$ recoveries with increasing elevation. Therefore, the $^{13}C$ recoveries increased distinctly between the lowest elevation (N01) and the highest located site (N05) (P=0.001, n=4). Furthermore, the recovered $^{13}C$ in the HF of the northern gradient also seemed to increase with increasing elevation. The $^{13}C$ recovery in the LF of the south-facing slopes showed constant values around 2% with the exception of site S09, which was slightly lower (Fig. 33). Despite the fact that the $^{13}C$ recovery stayed constant at the southern gradient, the $^{13}C$ recovery of the HF seemed to decrease with increasing altitude. Between the site S06 (1200 m a.s.l.) and S10 (2400 m a.s.l.) the recovered $^{13}C$ decreased distinctly by 1.2 % (P=0.031, n=4). At the sites S06, S07 and S08 the $^{13}C$ recoveries were balanced between the LF and HF (Fig. 32, Fig. 33). At higher altitudes of the southern gradient (1950 and 2400 m a.s.l.) the $^{13}C$ recovered in the HF decreased compared to the $^{13}C$ recovery in the LF. Both gradients revealed a shift from HF-dominated $^{13}C$ recoveries at the forest sites (1200, 1400 and 1650 m a.s.l.) toward LF-dominated $^{13}C$ recoveries at the grassland sites (1950 and 2400 m a.s.l.). Generally, this characteristic was more pronounced at southern gradient. Above all, the $^{13}C$ recoveries increased in the LF as well as in the HF with increasing elevation at the northern altitudinal gradient; the southern gradient was characterized by almost constant $^{13}C$ recoveries in the LF and declining $^{13}C$ recoveries upwards the gradient in the HF. The LF of the northern gradient exhibited significantly lower $^{13}C$ recoveries than the southern gradient, while the HF was not affected by significant differences in $^{13}C$ recoveries among both gradients.

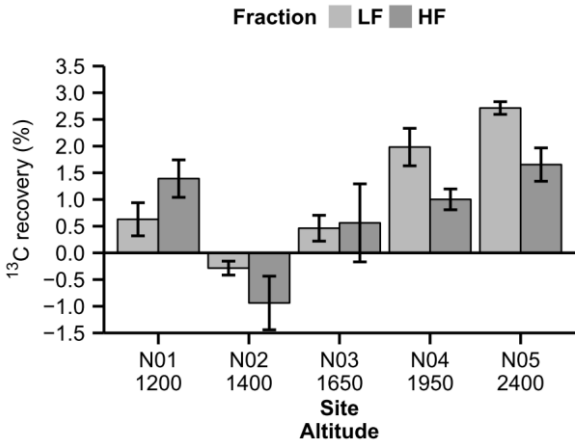


Fig. 32. Fraction-dependent $^{13}$C recoveries of the northern altitudinal gradient (0-5 cm).

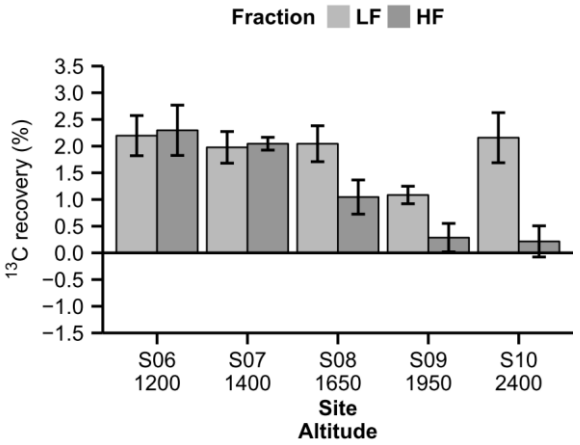


Fig. 33. Fraction-dependent $^{13}$C recoveries of the southern altitudinal gradient (0-5 cm).

Using the diluted $\delta^{13}$C signal of the mixed soil sample with the substrate for the term $\delta^{13}C_{substrate}$ in formula (3) led to distinctly higher $^{13}$C recoveries for all analyzed sites (Fig. 34, Fig. 35). The site-specific $^{13}$C recoveries only changed marginally in their relative distribution along the northern gradient compared to the uncorrected $^{13}$C recoveries (Fig. 32). Meanwhile, the southern gradient was characterized by rather heterogeneous $^{13}$C recoveries in both fractions. The southern gradient showed different $^{13}$C recovery trends compared to the uncorrected $^{13}$C recoveries (Fig. 35). The mean $^{13}$C recovery of the northern gradient accounted for 13.01 ± 4.00 % in the LF and for 9.13 ± 3.04 % in the HF. Meanwhile, the mean $^{13}$C recovery of the south-facing sites amounted to 25.22 ± 4.03 % in the LF and to 8.33 ± 2.17 % in the HF. The comparison of the $^{13}$C recoveries along both gradients showed that the mean $^{13}$C recovery of the LF at the northern gradient was significantly ($p=0.005$, $n=20$) lower than the mean $^{13}$C recovery of the LF at southern gradient. The $^{13}$C recoveries of the HF were not affected by significant exposition-specific influences.

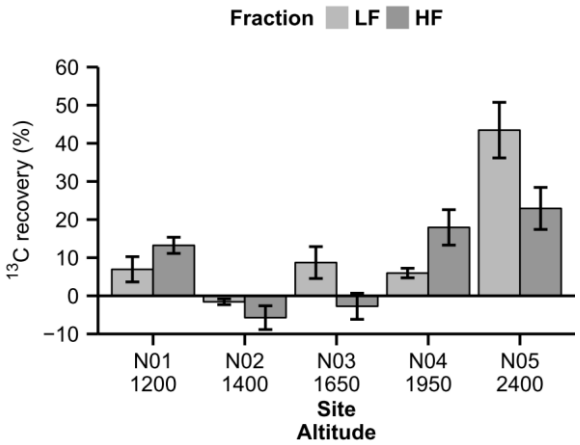


Fig. 34. Fraction-dependent $^{13}$C recoveries (diluted substrate) of the northern altitudinal gradient (0-5 cm)

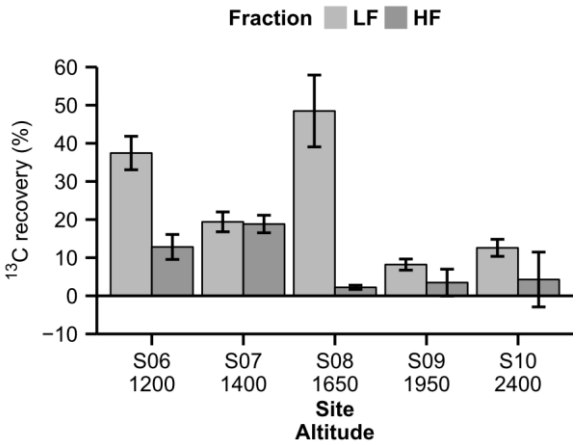


Fig. 35. Fraction-dependent $^{13}$C recoveries (diluted substrate) of the southern altitudinal gradient (0-5 cm)

Table 4
Chemical and physical characteristics of the density fractions of the 0-5 cm soil depth, n=[a,b], (mean (SE))

| Plot | Fraction | Mass percentage[a] (%) | C distribution[a] (%) | N distribution[a] (%) | SOC[a] ($g\ kg^{-1}$) | $N_{tot}$[a] ($g\ kg^{-1}$) | C/N ratio[a] | $\delta^{13}C$ control[b] (‰) | $\delta^{13}C$ label[b] (‰) | $^{13}C$ recovery[b] (%) | $^{13}C$ recovery (diluted substrate)[b] (%) |
|---|---|---|---|---|---|---|---|---|---|---|---|
| N01 | LF | 23.6 (5.6) | 62.8 (5.7) | 49.4 (6.9) | 437.3 (40) | 14.45 (0.50) | 30.50 (1.10) | -28.00 (0.15) | -27.55 (0.10) | 0.63 (0.31) | 6.95 (3.31) |
| N01 | HF | 76.4 (5.6) | 37.2 (5.7) | 50.6 (6.9) | 61.9 (6.55) | 3.79 (0.29) | 16.13 (0.53) | -26.75 (0.03) | -25.78 (0.24) | 1.39 (0.35) | 13.24 (2.12) |
| N02 | LF | 51.9 (14.3) | 73.6 (8.4) | 65.0 (11.2) | 434.2 (14.52) | 13.29 (1.12) | 34.39 (3.20) | -26.78 (0.03) | -26.98 (0.09) | -0.29 (0.13) | -1.58 (0.75) |
| N02 | HF | 48.1 (14.3) | 26.4 (8.4) | 35.0 (11.2) | 117.8 (29.23) | 6.35 (1.41) | 18.50 (1.30) | -26.13 (0.13) | -26.78 (0.26) | -0.94 (0.50) | -5.73 (3.12) |
| N03 | LF | 57.4 (13.2) | 77.6 (8.5) | 66.3 (10.4) | 462.8 (6.79) | 12.41 (0.69) | 38.40 (2.93) | -26.95 (0.09) | -26.63 (0.13) | 0.46 (0.24) | 8.72 (4.18) |
| N03 | HF | 42.6 (13.2) | 22.4 (8.5) | 33.7 (10.4) | 181.3 (30.25) | 8.38 (1.51) | 22.93 (2.53) | -26.33 (0.43) | -25.93 (0.21) | 0.56 (0.73) | -2.74 (3.42) |
| N04 | LF | 3.2 (0.6) | 15.1 (2.1) | 11.2 (1.4) | 418.5 (4.64) | 23.88 (1.40) | 18.07 (1.35) | -27.30 (0.09) | -25.90 (0.23) | 1.98 (0.35) | 5.97 (1.26) |
| N04 | HF | 96.8 (0.6) | 84.9 (2.1) | 88.8 (1.4) | 77.3 (7.44) | 6.05 (0.53) | 12.78 (0.64) | -26.55 (0.06) | -25.85 (0.19) | 1.00 (0.19) | 17.94 (4.64) |
| N05 | LF | 23.5 (3.0) | 50.6 (3.6) | 41.8 (4.0) | 447.1 (3.48) | 17.54 (0.45) | 25.61 (0.64) | -27.63 (0.05) | -25.70 (0.04) | 2.71 (0.12) | 43.46 (7.29) |
| N05 | HF | 76.5 (3.0) | 49.4 (3.6) | 58.2 (4.0) | 132.9 (11.24) | 7.41 (0.66) | 17.96 (0.17) | -26.18 (0.10) | -25.03 (0.17) | 1.65 (0.31) | 22.93 (5.51) |
| S06 | LF | 24.3 (3.7) | 77.1 (2.2) | 65.5 (3.3) | 432.3 (2.65) | 16.61 (0.32) | 26.09 (0.55) | -27.25 (0.06) | -25.70 (0.24) | 2.20 (0.38) | 37.45 (4.39) |
| S06 | HF | 75.7 (3.7) | 22.9 (2.2) | 34.5 (3.3) | 39.2 (5.86) | 2.66 (0.32) | 14.33 (0.49) | -26.33 (0.10) | -24.73 (0.28) | 2.30 (0.47) | 12.82 (3.27) |
| S07 | LF | 21.6 (4.5) | 64.3 (6.5) | 59.3 (6.6) | 401.0 (9.01) | 14.63 (0.46) | 27.54 (0.75) | -27.43 (0.19) | -26.03 (0.08) | 1.98 (0.30) | 19.40 (2.60) |
| S07 | HF | 78.4 (4.5) | 35.7 (6.5) | 40.7 (6.6) | 46.0 (6.57) | 2.44 (0.32) | 18.73 (0.63) | -26.35 (0.13) | -24.93 (0.09) | 2.05 (0.12) | 18.83 (2.30) |
| S08 | LF | 41.4 (9.2) | 78.4 (8.5) | 65.6 (10.1) | 446.0 (2.58) | 14.18 (0.36) | 31.61 (0.86) | -27.58 (0.13) | -26.13 (0.21) | 2.04 (0.34) | 48.48 (9.42) |
| S08 | HF | 58.6 (9.2) | 21.6 (8.5) | 34.4 (10.1) | 60.7 (10.71) | 3.39 (0.40) | 17.27 (0.95) | -26.05 (0.06) | -25.33 (0.28) | 1.05 (0.32) | 2.22 (0.56) |
| S09 | LF | 12.6 (1.4) | 35.6 (2.5) | 28.5 (2.3) | 422.0 (2.38) | 19.23 (0.37) | 22.02 (0.49) | -28.13 (0.11) | -27.35 (0.10) | 1.08 (0.16) | 8.20 (1.45) |
| S09 | HF | 87,4 (1.4) | 64.4 (2.5) | 71.5 (2.3) | 103.1 (7.99) | 6.85 (0.44) | 15.00 (0.29) | -26.60 (0.12) | -26.40 (0.14) | 0.29 (0.27) | 3.47 (3.51) |
| S10 | LF | 5.2 (1.1) | 13.9 (1.9) | 10.1 (1.7) | 415.6 (5.13) | 18.61 (0.59) | 22.51 (0.87) | -27.28 (0.15) | -25.75 (0.22) | 2.16 (0.47) | 12.59 (2.24) |
| S10 | HF | 94.8 (1.1) | 86.1 (1.9) | 89.9 (1.7) | 139.0 (11.45) | 8.70 (0.67) | 15.95 (0.17) | -26.00 (0.13) | -25.85 (0.09) | 0.21 (0.29) | 4.28 (7.19) |

[a] n=8, [b] n=4

# 4 Discussion

## 4.1 Bulk soil

***Soil temperature***

The soil temperature of the northern gradient decreased steadily with increasing elevation. This is exactly how temperature is expected to develop along an altitudinal gradient (Schaetzl and Anderson, 2005). Garten et al. (1999) reported a similar temperature regime at their investigated altitudinal gradient in the Appalachian Mountains. Although, the soil temperatures of the southern gradient were strongly variable along the toposequence, they generally decreased with increasing altitude. All north-exposed sites were characterized by significantly cooler soil temperatures than the south-exposed sites. These measurements coincide with energy balance models (EBM) (Gruber et al., 2004). It is widely accepted that microbial activity and, therefore, SOM decomposition is temperature dependent (Davidson and Janssens, 2006; Kirschbaum, 1995; Sierra, 2012). Van t'Hoff and colleagues found in early experiments that the reaction rates are changing with temperature according to following equation:

$$Resp = \alpha * e^{\beta T} \quad (8)$$

where *Resp* means soil respiration, α and δ are fitting parameter and *T* represents the Temperature (Davidson and Janssens, 2006; Davidson et al., 2006). Emerging from this formula several adaptations were used by different researchers leading to the rule of thumb that under standard conditions the SOM decomposition rate doubles or triples whenever there is an increase in temperature of 10°C (Davidson and Janssens, 2006). For the northern elevation gradient this means that the SOM decomposition rate should decrease with increasing elevation due to declining temperature with increasing elevation. Assuming that most of the not recovered $^{13}C$ was lost because of soil respiration (minor amounts due to DOC leaching) then the site-specific $^{13}C$ recoveries are expected to rise with increasing altitude since the recovered $^{13}C$ normally increases when soil respiration decreases. Similar trends can be observed at the northern gradient, where the $^{13}C$ recovery rises towards the highest elevated site. However, the southern altitudinal gradient rather revealed declining $^{13}C$ recoveries with increasing elevation (Fig. 14, Fig. 15). The correlation analysis between soil temperature and $^{13}C$ recovery confirmed a trend of increasing $^{13}C$ recoveries with decreasing soil temperature at the northern gradient ($R=-0.92$, $p<0.05$, $n=5$) (Table 5). The southern gradient did not follow this pattern. Similarly, Davidson and Janssens (2006) argue that SOM decomposition (and therefore also $^{13}C$ recovery) must experience other constraints than temperature as well.

***SOC concentration***

Altitude and exposure specific SOC concentration can help to interpret SOC stocks and site-specific $^{13}C$ recoveries. Both altitudinal sequences exhibited rather high SOC concentrations and showed strongly varying SOC concentrations. However, the high SOC concentration can also be explained through the sampling process. In order to avoid losing labeled material only the litter layer was removed and many samples contained pronounced Of and Oh horizons and therefore the SOC concentration of the upper 0-5 cm reached high SOC concentrations in some samples. Nevertheless, high and varying SOC concentrations are typical for forest soils as a result of local-scale variability in the soil environment of forest soils (Egli et al., 2009, 2006; Garcia-Pausas et al., 2007; Garten et al., 1999). The measured SOC concentrations comply with the measurements of Bardelli (2013) who

measured similar SOC concentrations at the same sites in different plots. Djukic et al. (2010) measured SOC concentration in the same magnitude at an altitudinal gradient in the Austrian Alps. Leifeld et al. (2009) reported for the Swiss Alps slightly lower SOC concentration along their altitudinal gradient. However, neither Djukic et al. (2010) nor Leifeld et al. (2009) considered different exposures in their gradients and therefore the SOC concentrations are not absolutely comparable.

The SOC concentration decreased with increasing soil depth (Fig. 5, Fig. 6). Interestingly, the SOC concentration of the northern altitudinal gradient rose continuously towards the altitude of 1650 m a.s.l. and declined again at the higher elevated sites. According to Egli et al. (2009) this regime of greatest SOC concentrations at the timberline is typical for Alpine regions. Meanwhile, the SOC concentrations at the southern gradient were rather constant at moderate altitudes, increased strongly towards the timberline (S08, 1650 m a.s.l.) and decreased slightly at higher altitudes. Garten et al. (1999) observed similar SOC concentration regimes along their altitudinal gradient. In contrast to this, Leifeld et al. (2009) measured continuously increasing SOC concentrations with increasing elevation in the upper 0-5 cm along their altitudinal gradient, however, the soil depths 5-10 and 10-15 cm again showed a maximum SOC concentration at medium elevation sites. Interestingly, the SOC concentration of the present study of upper 0-5 cm of the north-facing gradient did not differ significantly from the SOC concentration of the south-facing sites, whereas the soil depth 5-10 and 10-15 cm exhibited differences in SOC concentrations between the two gradients on a level of significance of p=0.1. An explanation for the lower SOC concentration at south-facing sites could be the faster SOM decomposition due to temperature-sensitive microbial activity (Davidson and Janssens, 2006).

***Nitrogen concentration***

All soil depths of both altitudinal gradients showed rising nitrogen concentrations with increasing altitude, while the nitrogen concentration increase of the 0-5 cm layer was characterized by abrupt increases of the nitrogen concentration (Fig. 7, Fig. 8). At the northern gradient the nitrogen concentration jumped between site N01 and N02 (Fig. 7) and at the southern gradient between S07 and S08 (Fig. 8). However, these trends of increasing nitrogen concentrations with increasing altitude were not statistically significant. The observed trends concur with the observation of Bardelli (2013) at the same sites. Nevertheless, Bardelli (2013) measured systematically higher and more variable nitrogen concentrations. An explanation for this shift between the present study and the nitrogen measurements of Bardelli (2013) could be that Bardelli (2013) included the litter layer in his 0-5 cm horizon. For instance, Bardelli (2013) measured in 0-5 cm soil depth nitrogen concentrations between 5.0 ± 1.1 and 21.0 ± 2.1 g N $kg^{-1}$, where our nitrogen concentrations varied between 5.9 ± 0.6 and 9.9 ± 1.5 g N $kg^{-1}$. However, Egli et al. (2006) measured even lower nitrogen concentrations at the same sites but it is to mention that they focused on the mineral soil. Zollinger et al. (2013) measured similar nitrogen concentrations at comparable altitudes and soil characteristics in the Swiss Alps. Powers (1990) and Rodeghiero and Cescatti (2005) found evidence that the soil nitrogen concentration is linked to soil temperature and soil moisture. Powers (1990) observed that nitrogen mineralization was greatest at medium elevations and was limited by temperature at higher elevations. Therefore, the nitrogen concentration is expected to be low at moderate altitude and high at more elevated sites. Comparable results were reported by Rodeghiero and Cescatti (2005) along their altitudinal gradient in the Italian Alps (Province of Trento). They found a correlation of R= -0.29 between soil temperature and nitrogen concentration in the soil, although this correlation was

not significant. Similar relations between soil temperature and nitrogen concentration can also be observed at the southern gradient in the 0-5 cm soil depth (R= -0.95, p=0.013, n=5) (Fig. 37). In contrast to this, the 0-5 cm soil depth of the northern gradient did not exhibit any significant relations between total nitrogen concentration and soil temperature (Fig. 36). Hence, Marrs et al. (1988) conclude that soil temperature is not the only factor controlling the total nitrogen concentration, especially soil structure and aeration can have a great influence on the overall nitrogen concentration as well.

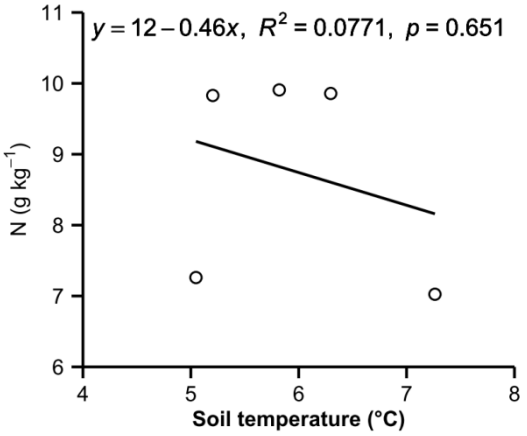


Fig. 36. Linear regression between total nitrogen concentration of the northern gradient (0-5 cm) and mean annual soil temperature

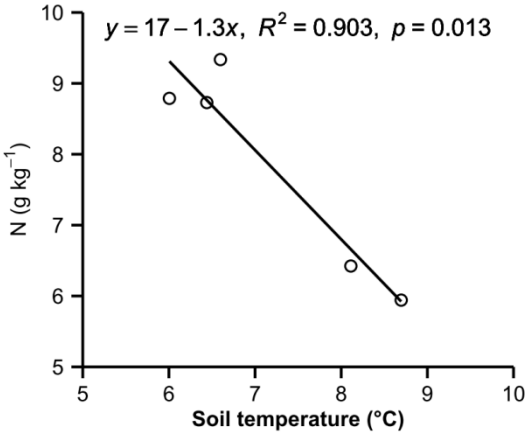


Fig. 37. Linear regression between total nitrogen concentration of the southern gradient (0-5 cm) and mean annual soil temperature

Table 5
Pearson correlation matrix of bulk soil parameters (northern altitudinal gradient) – bold values indicate significant correlations (p≤0.05), n=5

| | Soil temp. | Sand | Silt | Clay | C/N ratio | $\delta^{13}C$ | $^{13}C$ recovery | $^{13}C$ recovery (diluted substrate) |
|---|---|---|---|---|---|---|---|---|
| Soil temp. | **1** | 0.06 | 0.62 | 0.35 | 0.26 | -0.08 | **-0.92** | **-0.92** |
| Sand | 0.06 | **1** | 0.36 | 0.39 | -0.75 | -0.73 | 0.30 | 0.27 |
| Silt | 0.62 | 0.36 | **1** | 0.84 | -0.05 | -0.07 | -0.56 | -0.51 |
| Clay | 0.35 | 0.39 | 0.84 | **1** | 0.14 | -0.40 | -0.26 | -0.15 |
| C/N ratio | 0.26 | -0.75 | -0.05 | 0.14 | **1** | 0.18 | -0.47 | -0.36 |
| $\delta^{13}C$ | -0.08 | -0.73 | -0.07 | -0.40 | 0.18 | **1** | -0.27 | -0.32 |
| $^{13}C$ recovery | **-0.92** | 0.30 | -0.56 | -0.26 | -0.47 | -0.27 | **1** | **0.99** |
| $^{13}C$ recovery (diluted substrate) | **-0.92** | 0.27 | -0.51 | -0.15 | -0.36 | -0.32 | **0.99** | **1** |

Table 6
Pearson correlation matrix of bulk soil parameters (southern altitudinal gradient) – bold values indicate significant correlations (p≤0.05), n=5

| | Soil temp. | Sand | Silt | Clay | C/N ratio | $\delta^{13}C$ | $^{13}C$ recovery | $^{13}C$ recovery (diluted substrate) |
|---|---|---|---|---|---|---|---|---|
| Soil temp. | **1** | -0.30 | 0.69 | -0.27 | 0.29 | -0.39 | 0.46 | 0.27 |
| Sand | -0.30 | **1** | 0.05 | -0.72 | 0.32 | 0.43 | 0.27 | 0.29 |
| Silt | 0.69 | 0.05 | **1** | -0.13 | 0.18 | 0.09 | 0.03 | -0.06 |
| Clay | -0.27 | -0.72 | -0.13 | **1** | -0.35 | -0.17 | -0.63 | -0.48 |
| C/N ratio | 0.29 | 0.32 | 0.18 | -0.35 | **1** | -0.68 | 0.85 | 0.94 |
| $\delta^{13}C$ | -0.39 | 0.43 | 0.09 | -0.17 | -0.68 | **1** | -0.66 | -0.72 |
| $^{13}C$ recovery | 0.46 | 0.27 | 0.03 | -0.63 | 0.85 | -0.66 | **1** | **0.96** |
| $^{13}C$ recovery (diluted substrate) | 0.27 | 0.29 | -0.06 | -0.48 | **0.94** | -0.72 | **0.96** | **1** |

***C/N ratio***

The C/N ratios at all investigated soil depths were very high, which is typical for sites with distinct O-horizons (Egli et al., 2009; Stahr et al., 2012). There was the tendency that the C/N ratios of both gradients were higher at medium altitudes, which were characterized by distinct organic horizons, compared to low- and high-elevated sites (Bardelli, 2013). According to Dahlgren et al. (1997) the C/N ratio rises with increasing altitude as this reflects increasing SOC concentration at higher elevations. However, it is often observed that the C/N ratio declines again at higher altitudes since the litter input often reaches its maximum at medium altitudes and declines at high elevated sites (Dahlgren et al., 1997). An explanation for the decreasing C/N ratios at higher altitude could be the shift from forest soils to grass-dominated soils. The magnitude of the C/N ratio was within the same range as Bardelli (2013) reported for the same area of investigation. Interestingly, Bardelli (2013) found rather continuous C/N ratios along both gradients, while our measurements indicated maximum C/N ratios at 1650 m a.s.l. and lower values at low- and high-elevated sites. Egli et al. (2009) measured slightly lower C/N ratios in the same area but they were investigating the mineral soil only.

The declining C/N ratios with increasing soil depth indicate that the SOC mineralization proceeds faster than the nitrogen mineralization (Stahr et al., 2012). The southern altitudinal gradient showed significantly (p=0.000, n=40) declining C/N ratios with increasing soil depth (Fig. 10), while the north-facing sites did not exhibit a clear trend (Fig. 9). Additionally, the C/N ratios of the southern gradient were significantly lower at the soil depth 5-10 and 10-15 cm compared to the north-facing sites. Thus, the C/N ratio may indicates that the SOC decomposition of the southern gradient could be benefitted (Garten et al., 2000; Stahr et al., 2012). Along the southern gradient the C/N ratio correlated significantly with the $^{13}C$ recovery of the bulk soil (R= 0.94, p=0.02, n=5) (Table 6), while at the northern gradient no significant correlation was observed. However, it is also important to investigate the soil coverage since plant species-dependent biomass characteristics can influence the C/N ratio (Stahr et al., 2012). Overall, the $^{13}C$ mineralization could be benefitted at the southern gradient since the C/N ratios were distinctly lower in the soil depths of 5-10 cm and 10-15 cm at the south-facing sites.

***SOC stocks***

The SOC stocks of the northern and southern gradient were similar to what was reported by Rodeghiero and Cescatti (2005) in the Italian Alps, Gracia-Pausas et al. (2007) in the Pyrenees, Dahlgren et al. (1997) in the western Sierra Nevada and Garten and Hanson (2006) in the Appalachian Mountains. Djukic et al. (2010) and Leifeld et al. (2009) reported slightly different SOC stocks in their investigated area due to different soil profile depths or different climatic conditions. A number of studies indicate rising SOC stocks with increasing altitudes (Garcia-Pausas et al., 2007; Garten and Hanson, 2006; Garten et al., 2000; Leifeld et al., 2009) but other researchers found increasing SOC stocks with increasing altitude with maximum SOC stocks at the tree line, followed by decreasing SOC stocks at higher altitude (Dahlgren et al., 1997; Djukic et al., 2010; Garten et al., 1999; Rodeghiero and Cescatti, 2005). On the on hand, Davidson and Janssens (2006) argue that higher SOC stocks at high altitudes can be explained by decreasing temperatures with increasing altitude, since a decline in temperature reduces microbial activity. The less SOM that is mineralized, the more SOM will be stored in the soil. On the other hand, Schmidt et al. (2011), but also Davidson and Janssens (2006), note that other constraints than temperature may influence SOC stocks. For instance, freezing processes and snow cover during wintertime can inhibit SOC accumulation (Garcia-Pausas et al., 2007).

The SOC stocks of the present investigation exemplified both regimes of SOC stocks along the altitudinal gradients. The northern altitudinal sequence was characterized by increasing SOC stocks toward mid-elevations, followed by a slight decrease in SOC concentration, while the southern gradient showed rising SOC stocks with increasing altitude (Fig. 11). An explanation for the different behavior of the SOC stocks along both gradients could be different soil covers at higher altitudes (Garcia-Pausas et al., 2007). In grassland soils, the proportion of SOC storage can be higher than in forest ecosystems due to a dense and carbon-rich root network in grassland soils (Garcia-Pausas et al., 2007). Similar observations were made at the sites N04, N05, S09 and S10. While the sites S09 and S10 were characterized by grassland with intense root networks, the sites N04 and N05 showed less dense grass coverage. Therefore, it seemed that the SOC stocks of the south-facing sites S09 and S10 were more influenced by carbon from root and shoot biomass. An additional explanation as to why the SOC stocks of the southern gradient did not decline at the high elevated sites can be derived from the skeleton data (Table 2). While the skeleton mass of the north-facing sites was rising with increasing altitude, the south exposed sites showed declining skeleton masses with increasing elevation. Although several soil properties changed along both altitudinal sequences, the magnitude of the SOC stocks of both gradients did not differ significantly along the gradients nor between the two aspects. Nevertheless, the SOC stocks were influenced by varying soil coverage, shifts in skeleton mass and probably by temperature changes along the altitudinal gradients as both gradients showed different SOC stocks regimes along the two gradients.

## 4.2 Isotopic signature, 13C recovery and priming effect of the bulk soil (0-5 cm)

***$\delta^{13}C$ signature***

Many studies were conducted to investigate how the $^{13}C$ signal of SOC develops along increasing soil depth. However, only few studies analyzed the variation of $^{13}C$ along altitudinal gradients previous to this investigation. It is widely accepted that vertical changes in $\delta^{13}C$ values are caused by isotopic fractionation during the decomposition of SOM and biomass characteristics (Garten et al., 2000). Especially, the initial litter quality and the properties of microbial decomposers community seem to be crucial for the vertical $\delta^{13}C$ characteristics in soil profiles (Garten et al., 2000). Moreover, it is of interest how the $\delta^{13}C$ composition develops along different elevations. Since the $\delta^{13}C$ signal of the SOM seems to depend on litter and plant species, Hultine and Marshall (2000) analyzed how plant-specific foliar $\delta^{13}C$ values varied along altitudinal gradients. According to their measurements the $\delta^{13}C$ values of *Picea* plants became significantly less negative with increasing altitude. Hence, it may be argued that the $\delta^{13}C$ signal of SOM increases with increasing altitude. The $\delta^{13}C$ isotopic ratios (soil) of the northern gradient coincide with the $\delta^{13}C$ signal of CWD measurements at the same sites (Petrillo et al., 2015). Petrillo et al. (2015) observed the most negative $\delta^{13}C$ signatures of the CWD at low and high elevated sites and the highest $\delta^{13}C$ composition of the CWD at the altitude of 1650 m a.s.l. Therefore, the present isotopic rations of the northern soils and the $\delta^{13}C$ measurements of CWD seem to reflect the observations of Hultine and Marshall (2000). The present isotopic signature of the southern altitudinal gradient showed similar $\delta^{13}C$ regimes like the $\delta^{13}C$ values reported by Garten et al. (2000) along their elevation gradient in the Appalachian Mountains, characterized by minimum negative $\delta^{13}C$ values at medium altitude. The northern altitudinal gradient exhibited inverse $\delta^{13}C$ signals compared to the southern gradient (Fig. 12, Fig. 13).

In contrast to this, Powers and Schlesinger (2002) reported in their experiment that the surface soil isotopic composition did not positively correlate with the isotopic signature of vegetation inputs at any level. All the more, the isotopic composition of the surface soil strongly correlated with topography and edaphic factors. Therefore, Powers and Schlesinger (2002) conclude that soil isotopic signature is linked to SOC turnover processes. Interestingly, Powers and Schlesinger (2002) found a negative correlation between $\delta^{13}C$ values of their soils and the C/N ratio ($R= -0.77$, $p<0.05$). The present data also exhibited for the southern gradient a negative correlation between the $\delta^{13}C$ signals and the C/N ratios ($R= -0.68$, $p>0.05$, $n=5$) (Table 6), whereas the northern gradient showed a positive correlation between these two variables. Furthermore, the $\delta^{13}C$ can be seen as indicator for SOM decomposition characteristics and it is possible that less negative $\delta^{13}C$ signatures may suggest more processed SOM (Bird et al., 2008). Moreover, the present isotopic data of the bulk soil showed a negative correlation between the $^{13}C$ recovery and the $\delta^{13}C$ signature along both gradients (northern gradient: $R= -0.32$, $p>0.06$; southern gradient: $R= -0.72$, $p>0.05$) (Table 5, Table 6). This observations support the hypothesis of Powers and Schlesinger (2002) who suppose that isotopic composition is related to SOC turnover processes.

***$^{13}$C recovery***

In the chapter entitled 'results', two different approaches were presented of how to calculate $^{13}$C recoveries that gave rise to rather divergent $^{13}$C recoveries. The consideration of dilution of the isotopic signature of the substrate trough the natural isotopic signature of the soil sample leads to significantly higher $^{13}$C recoveries than without taking dilution into account. The main difficulties in evaluating both resulting $^{13}$C recoveries are diverse approaches concerning the determination of the substrate/$^{13}$C recoveries (isotope labeling approaches, litter bag approaches, combining litter bag approaches with labeled substrate), different applied substrates (different plant species, different plant material (roots, leaves, braches)), different apparent climatic conditions at the areas of investigation and that only a few studies were conducted along altitudinal gradients. Additionally, most of the studies investigate SOM decomposition by conducting measurements of soil respiration and DOC leaching. The reported $^{13}$C recoveries of both approaches differ approximately by a factor of 20.

Table 7
Overview about different litter decomposition studies

| Author | Location | Method | Substrate | time span | Results |
|---|---|---|---|---|---|
| Present Study | Trentino, Italy | Stable isotopes | Norway spruce needles | 12 month | 25.1 ± 6.99 %, 34.7 ± 4.77 % (diluted substrate) |
| Bird et al. (2008) | Sierra Nevada, USA | Stable isotopes | Pine needles | 24 month | 18.1 ± 2.7 % |
| Bottner et al. (2000) | France | Stable isotopes | Wheat residues | 12 month | 35% |
| Rubino et al. (2010) | Tuscania, Italy | Stable isotopes | Black poplar foliage | 11 month | 20.0 ± 3.0 % |
| Kammer and Hagedorn (2011) | Lägern, Switscherland | Stable isotopes | Beech foliage | 12 month | 23-31 % |
| Kammer and Hagedorn (2011) | Lägern, Switscherland | Litter bag (mass loss) | Beech foliage | 12 month | 67.50% |
| Murphy et al. (1998) | Arizona, USA | Litter bag (mass loss) | different Pine needles | 12 month | 75-85 % |
| Lorenz et al. (2000) | Black Forest, Germany | Litter bag (mass loss) | Norway spruce needles | 12 month | 77.5 ± 2.4 % |
| Lorenz et al. (2000) | Ontario, Canada | Litter bag (mass loss) | Norway spruce needles | 12 month | 78.6 ± 4.4 % |

Overall, several studies concerning litter decomposition were conducted (Table 7). One comparable study was conducted by Bird et al. (2008) in the Sierra Nevada which is closely related to our study since they used $^{13}$C labeled pine needles. Their study was carried out in Mediterranean climate. Bird et al. (2008) reported $^{13}$C recoveries of 18.1 ± 2.7 % in the bulk soil after two years. Another comparable study was conducted by Bottner et al. (2000) who investigated litter decomposition along European soils. The advantages of this study are climatic conditions similar to the soils of Italy, comparable soil coverage (for some sites *Picea Abies*) and a comparable experimental setup. Nevertheless, the comparability is still restricted since another substrate was used (wheat). Bottner et al. (2000) reported $^{13}$C recoveries after one year of approximately 35% for their soil analysis in France. Another $^{13}$C litter labeling experiment was performed by Rubino et al. (2010) in Italy

(Tuscania) where labeled black poplar (*Populus nigra)* foliage was used. Rubino et al. (2010) reported litter losses of 80.0 ± 3.0 % of the initial substrate. Kammer and Hagedorn (2011) conducted a litter labeling experiment in Switzerland at the south-facing slope of the Lägern mountain. The major differences to the present study were the varying litter material (beech foliage), the $^{13}C$ label that was achieved by depletion ($\delta^{13}C$ = -40.4), the litter substrate which was added as litter layer and not below the litter layer (as it was done in the present study) and finally, the different parent material, namely marl. Under these conditions, Kammer and Hagedorn (2011) measured mean $^{13}C$ recovery of 23-31 % after one year.

It was of great advantage that Kammer and Hagedorn (2011) additionally investigated the leaf litter decomposition in litter bags in order to evaluate the difference between isotopic label and litter bag experiments. They found that litter bags had twice to three times higher substrate recoveries compared to the isotope labeling approaches. This is interesting since other data on substrate recovery are available from litter bag experiments. Murphy et al. (1998) conducted a litter bag experiment along an altitudinal gradient in the area of northern Arizona. The site is characterized by a semi-arid climate and is dominated by pine trees (*Pinus edulis* and *Pinus ponderosa).* Murphy et al. (1998) reported litter mass recovery of approximately 75-85 % after one year of field application. It is important to mention that they measured mass recovery and not carbon or $^{13}C$ recovery. However, the relevant aspects of their work for the present study are the relative changes in substrate recoveries along their gradient. Murphy et al. (1998) noticed declining litter mass recovery with increasing altitudes. Similar observations were reported in the present study of the southern altitudinal gradient. Lorenz et al. (2000) also investigated mass loss experiments with litter bags. The advantages of their study in relation to the present work are the use of Norway spruce needles and comparable climatic conditions. Their experiments took place in Germany (Black Forest) and Canada (northern Ontario). Lorenz et al. (2000) found rather similar litter mass recoveries for Germany and Canada after 10 respectively 12 months, namely 77.5 ± 2.4 % and 78.6 ± 4.4 % respectively. The present average $^{13}C$ recoveries of the north-facing sites of 0.8 ± 0.21 % and at the south- facing sites of 1.5 ± 0.19 % seem to be distinctly lower than the $^{13}C$ recoveries by Bird et al. (2008), Bottner et al. (2000) and Kammer and Hagedorn (2011). The $^{13}C$ recoveries under consideration of substrate dilution thus predominately coincide with the magnitude of the results from the researchers mentioned. On the other hand, the present experiment was conducted with milled Norway spruce needles, whereas the other experiments were performed with native plant material. The comparability of the litter bag experiments is low since most of the litter bag experiments focus on mass loss and not on carbon/$^{13}C$ loss. As Kammer and Hagedorn (2011) reported it is possible that the litter bags may harm litter decomposition due to the presence of a mesh between the plant residues and the soil. If the results of the litter bag experiments are corrected with the factor observed by Kammer and Hagedorn (2011), then the substrate recoveries will be in the same range as those from the isotopic labeling experiments. Another problem arises because most researchers did not indicate whether they took into account the dilution of the isotopic signature of the substrate by the isotopic composition of the soil or not. Therefore, both approaches to calculate the $^{13}C$ recovery were performed.

***$^{13}$C recovery along the climosequence***

The assessment of the presented $^{13}$C recoveries in relation to the climosequence revealed some interesting results. The first surprising observation is that the average $^{13}$C recovery at the northern altitudinal gradient was lower than at the southern gradient (Fig. 15). According to Davidson and Janssens (2006), the decomposition of SOM is expected to be higher at elevated temperatures due to a positive relation between temperature and microbial activity in the soil. Therefore, the $^{13}$C recovery is expected to be lower at locations with higher soil temperatures as soil microorganisms mineralize more SOM to $CO_2$ in higher temperatures (Davidson and Janssens, 2006; Garten and Hanson, 2006). Furthermore, the significantly lower C/N ratio of the southern gradient and also the slightly higher SOC stocks of the northern gradient indicate theoretically pronounced mineralization of SOM and lower $^{13}$C recoveries at the southern gradient. Despite these indicators, the $^{13}$C recovery trends are reversed. A possible explanation can be found in exposure-specific differences in plant detritus inputs or differences in soil moisture (Davidson and Janssens, 2006). The present data about soil moisture (measured at the date of sampling) indicates distinctly lower soil moisture in the 0-5 cm soil depth ($p=0.006$, $n=20$) (Table 2) at the southern altitudinal gradient compared to the northern gradient. Also, Bardelli (2013) measured soil moisture in the same range and with the same manifestation of lower soil moisture at the south-facing sites. This raises the question of whether the soil moisture was low enough to harm SOC decomposition at the southern gradient. Unfortunately, it is not possible to answer this question with the present investigations.

Along both gradients special pattern of $^{13}$C recoveries occurred. Jenny et al. (1949) observed that litter input and SOM decomposition are highest at mid-elevated sites of an altitudinal gradient (Dahlgren et al., 1997; Garten and Hanson, 2006). Similar characteristics can be found at the northern elevation gradient, where the lowest $^{13}$C recoveries were observed at medium elevated sites (Fig. 15). The southern gradient showed more complex $^{13}$C recovery dynamics. It seemed that the $^{13}$C recoveries were falling with increasing elevation toward mid-elevated sites followed by a week increase of $^{13}$C recovery at high-elevated sites (Fig. 15). Interestingly, the altitude of 1650 m a.s.l., where the lowest $^{13}$C recovery is expected (Jenny et al., 1949), revealed the highest $^{13}$C recovery of the southern gradient. Furthermore, the high elevated sites S09 and S10 showed rather low $^{13}$C recoveries. Therefore, it seems that the $^{13}$C recoveries of the northern gradient coincide more with the observations of Jenny et al. (1949), whereas the $^{13}$C recoveries showed an analogy to the experiment of Murphy et al. (1998). An explanation for these observations can be found in the fact that the high elevated sites of the southern gradient were characterized by intense grass coverage with low humus horizons (Bardelli, 2013). For a better understanding of the litter decomposition characteristics it would be important to measure $^{13}$C recoveries in the minerals soil as well. Overall, the $^{13}$C recoveries of 0-5 cm soil depth coincide well with the isotopic composition, the C/N ratio and soil temperature of the bulk soil along the altitudinal gradients, whereas the exposure-specific 13C recoveries are difficult to explain. However, the SOM decomposition seems to be a combination of local (litter quality, litter input, soil moisture, C/N ratio) and global (temperature and precipitation) environmental factors (Dahlgren et al., 1997; Garten and Hanson, 2006).

***Priming effect***

The priming effect of the northern gradient was positive which means that the SOM decomposition was inhibited, while the negative PE of the southern gradient indicates induced SOM decomposition (Fig. 16) (Fontaine et al., 2004). The PE characterizes an extra decomposition of SOC after addition of an easily decomposable substrate to the soil due to stimulated mineralization caused trough soil microorganisms (Kuzyakov et al., 2000). Depending on the substrate added it is possible that the supply of degradable SOM increases the SOM feeding microbes population, which can survive even after the substrate was exhausted (Fontaine et al., 2004). Thus, it may be possible that the increased microbe population degrades more SOM than under natural soil conditions. In contrast to this, it could also be that the inexpedient substrate inhibits SOM decomposition (Fontaine et al., 2004). In both cases the SOM characteristics differ compared to natural soil characteristics. If the PE is negative, then the substrate input to the soil decreases the total SOC and if the PE is positive, then the substrate increases total SOC of the soil (Fontaine et al., 2004). The PE of the present study was rather heterogeneous along the gradients and, therefore, it is possible that measurement inaccuracy or the heterogeneity of the alpine soil properties caused the apparent PE. On the one hand, the sensitivity analysis exhibited that a change in SOC concentration of 1% can cause a variation in the PE of 2%. On the other hand, it became apparent during the soil sampling that soil characteristics changed on very small scale. Although control and labeled plots were located close to each other, it was possible that different soil properties were found. Therefore, we assume that the addition of 1.4-2 g of substrate cannot cause a difference in SOC concentration of 68.2 ± 34.9 g $kg^{-1}$ (northern gradient) and -57.6 ± 16.8 g $kg^{-1}$ (southern gradient) respectively, between control and labeled plots.

## 4.3 Density fractionation (0-5 cm)

***Fraction-dependent soil mass, carbon and nitrogen distribution***

In order to investigate further factors controlling SOM decomposition and stabilization the soil samples were separated into a LF and HF. Beside litter quality, litter input, soil moisture, C/N ratio, temperature and precipitation, physical protection of OM and chemical binding of organic molecules to mineral surfaces can also influence SOM decomposition (Davidson and Janssens, 2006; Schmidt et al., 2011). The mass and carbon recovery after the density fractionation lay within the same range as reported by Glaser et al. (2000) , Cerli et al. (2012) or Schrumpf et al. (2013). Large amounts of the soil mass were found in the HF, especially at the high-elevated grass-dominated sites (Fig. 17). Meanwhile, the LF showed maximum amounts of the soil mass at mid-elevated sites. Since the calculation of the fraction dependent C distribution is strongly influenced by the fraction mass, similar trends can be observed for the mass corrected carbon distribution among the LF and HF. The LF of the mid-elevated sites showed the highest carbon contents at both gradients while at low and high elevated sites more carbon was found in the HF (Fig. 22). Similar observations were also valid for the nitrogen distribution along the northern and southern altitudinal gradients. However, the magnitudes of the nitrogen distribution differed from those of the OC distribution. Along both gradients more nitrogen was found in the HF (Fig. 23), while OC distribution showed maximum amounts in the LF. In sum, it is to mention that more OC was encountered in the LF, whereas more nitrogen was found in the HF.

***Density-dependent SOC concentration***

The SOC concentrations in the LF were rather constant on a high level (northern gradient: 440.0 ± 5.7 g $kg^{-1}$; southern gradient: 423.4 ± 4.6 g $kg^{-1}$). These observations showed analogous magnitudes to Christensen (2001) described as typical values for OM concentrations in the LF. Furthermore, the organic matter in the HF was significantly less concentrated than in the LF and showed rising concentrations with increasing altitude (Fig. 18, Fig. 19). Similar trends for the LF and HF SOC concentrations were reported along the altitudinal gradient of Wagai et al. (2008). Sollins et al. (2006) assume that the SOC concentration decreases with increasing particle density of the soil fraction. This assumption is valid for all investigated fractions along both gradients. Lützow et al. (2007) explain the extreme low SOC concentration in the HF by means of low mineral content in the O-horizon. In contrast to this, the LF was characterized by high SOC concentration.

***Total nitrogen concentration of the density fractions***

The nitrogen concentration of the LF decreased with increasing altitude for both altitudinal gradients (Fig. 20, Fig. 21). However, the decline was interrupted by an abrupt drop of the nitrogen concentration between 1650 and 1950 m a.s.l. This drop of the nitrogen concentration in the LF may have occurred due to changes in vegetation or because of changes in mineral composition at the transition from forest soil to a more open forest intersected grassland soils. This hypothesis is supported by the fact that the low density fraction of the O-horizon is commonly influenced by plant detritus (Christensen, 2001; von Lützow et al., 2007). The nitrogen concentrations of the LF and the HF of both gradients were within the same range as reported by Hatton et al. (2012), Wagai et al. (2008) or Sollins et al. (2006). In their fractionation experiments, Sollins et al. (2006) and Hatton et al. (2012) observed that the nitrogen concentration decreased with increasing soil density. The LF and HF of the present experiment showed similar characteristics. The nitrogen concentration decreased significantly along the transition from the LF to the HF.

***C/N ratio***

The C/N ratios were in the same range as Gunina and Kuzyakov (2014) measured in the O-horizon of European forest soils, Bird et al. (2008) reported in forest soils in the Sierra Nevada and Wagai et al. (2008) and Graten et al. (1999) measured along their altitudinal gradients. Wagai et al. (2008) and Garten et al. (1999) observed increasing C/N rations in the LF as well as in the HF with increasing altitude. Similar regimes for C/N ratios can be found in the present study, although only for the forest sites (N01-N03 and S06-S08) (Fig. 24, Fig. 25). Thereafter, the C/N ratio dropped distinctly in both fractions. This drop in C/N ratio is caused by a significant increase in fraction-dependent nitrogen concentration at the grass dominated sites (1950 and 2400 m a.s.l.).

The fraction-dependent C/N ratio is a helpful tool for assessing fraction-specific SOM decomposition and stabilization. On the on hand, Hatton et al. (2012) argue that the decrease from high C/N ratios in the LF to low C/N ratios in the HF can be interpreted as a change from unprocessed plant material, dominated by OM in the LF, towards processed microbial characterized OM in the HF. Evidence for such a shift can be gained from different $^{13}C$ and $^{15}N$ isotopic abundance between low density and high density soil fractions (Hatton et al., 2012). According to Hatton et al. (2012) and Kleber et al. (2007) especially microbial derived nitrogen decomposition products and proteinaceous microbial residues have a high affinity to bind to mineral surfaces of the dense soil fractions. Meanwhile, the C/N ratio of the lightest fraction (<1.6 g $cm^{-3}$) is characterized by high C/N ratios because of the strong influence of carbon rich plant residues (Sollins et al., 2006). Therefore, it can be interesting to analyze the differences of the C/N ratio between the LF and the HF per sampling site in order to derive information about SOM decomposition. Decreasing C/N ratios with increasing fraction density were observed for all sites (Fig. 24, Fig. 25) in the present study as Hatton et al. (2012), Sollins et al. (2006) or Gunina and Kuzyakov (2014) already reported previously. On average, the C/N ratios differed more between the LF and HF at the northern gradient. Hence, the SOM decomposition may be higher at the northern gradient compared to the southern gradient.

***Isotopic carbon signature***

Stable isotope ($^{13}C$) tracers in combination with a SOM density fractionation approach can be used to investigate stabilization and decomposition of SOM among different SOM pools and pathways (Bird et al., 2008). However, in a first attempt it is of interest to assess the natural isotopic abundance along both altitudinal gradients and within density fractions. The investigated fraction-dependent $\delta^{13}C$ signals were slightly more negative than what Bird et al. (2008) reported from coniferous forest soils in the Sierra Nevada but comparable to European forested sites, investigated by Hatton et al. (2012) (beech forest) or Gunina and Kuzyakov (2014) (Norway spruce forest). Based on natural abundance of the fraction-specific isotopic composition it is possible to derive SOM decomposition characteristics (Bird et al., 2008). On the on hand, several studies indicate that the $\delta^{13}C$ signal increases (become less negative) with increasing particle density (Bird et al., 2008; Gunina and Kuzyakov, 2014; Hatton et al., 2012). The present study also reported distinctly more negative $\delta^{13}C$ values for the LF compared to the HF (Fig. 26, Fig, 27, Fig. 28, Fig. 29). Gunina and Kuzyakov (2014) explain the differences in the isotopic signature among different particle density by means of stabilization of OM after passing one or more microbial degradation cycles. The differences in the isotopic signature occur due to isotopic discrimination during the microbial decomposition process. Microorganisms preferentially use the lighter $^{12}C$ isotope of the OM, which needs less kinetic energy during mineralization, than the heavier $^{13}C$ isotope of the OM (Glaser et al., 2000; Powers and Schlesinger, 2002). It is supposed that the degraded $^{13}C$ enriched OM is by trend stabilized in the HF,

which normally exhibits higher mineral contents with higher chemical binding capacity than the LF (Hatton et al., 2012). The $\delta^{13}C$ signal in the HF of all control sites was rather constant and significantly less negative than $\delta^{13}C$ signal in the LF. Hence, the $\delta^{13}C$ ratios of the HF indicate that microbial degraded SOM is available in the HF and potentially stabilized by means of binding to silt and clay particles in the 0-5 cm soil depth.

To evaluate the absolute SOC fluxes between the litter and the soil fractions as well as the decomposition rate of the applied litter it is necessary to also take into account the isotopic signature of the labeled soil samples. According to formula (3) it is possible to calculate how much of the initial litter substrate is recovered in which soil compartments. The more the $\delta^{13}C$ signal of the control and labeled sample per site and fraction is digressing, the more $^{13}C$ will be recovered. The LF was characterized by significant differences between control and labeled soil at the sites N04, N05, S06, S07, S08, S09 and S10 (Fig. 26, Fig. 27). At these sites, the applied substrate seemed to decompose more slowly than at the remaining sites. For the HF, large substrate recoveries are expected at the sites N05, S06 and S07 (Fig. 28, Fig. 29). The $\delta^{13}C$ differences between control and labeled plots of the other sites indicate fast SOM decomposition and low SOC stabilization in the HF. An interesting artifact can be observed at the site N02 where the $\delta^{13}C$ signature of the labeled sample was more negative in both density fractions as the $\delta^{13}C$ signal of the control sample (Fig. 26, Fig. 28). This circumstance is theoretically not possible since this isotopic signature indicates substrate production, which is not reasonable. Therefore, the differences are small and probably a consequence of measuring inaccuracy and we assume a substrate recovery of 0 for this site.

***Fraction-dependent isotopic nitrogen composition***

The nitrogen isotopic signature of the control soil (LF and HF) showed a rather heterogeneous trend along both elevation gradients. The HF of the southern gradient exhibited rising $\delta^{15}N$ values with increasing altitude. For the $\delta^{15}N$ values of the LF of the southern gradient and the LF as well as the HF of the northern gradient, no clear trends were observable. The measured $\delta^{15}N$ signals lay within the same range as Hatton et al. (2012) reported in their experiment. According to the gradient-specific mean $\delta^{15}N$ values of the LF and HF it seemed that the $\delta^{15}N$ ratio of the northern gradient was less negative than the $\delta^{15}N$ signatures of the southern gradient (Fig. 30, Fig. 31). Furthermore, increasing $\delta^{15}N$ signatures were observed with increasing particle density. Similar observations were reported by Hatton et al. (2012). The $\delta^{15}N$ signal between the LF and HF differed more at the northern altitudinal gradient, although generally only marginal differences occurred. An explanation for the $^{15}N$ enrichment in the HF could be the discrimination of $^{15}N$ during the decomposition process of microorganisms (Huygens et al., 2008). A possible scenario was proposed by Hatton et al. (2012) who explain the $^{15}N$ enrichment in the dense soil fractions as a result of microbial processed OM and its adsorption through reactive mineral surfaces of the dense soil fractions. More precisely, the decomposition product $^{15}NH_4^+$ is often found interacting with negatively charged mineral compounds in acidic environment of the dense soil fraction (Hatton et al., 2012). Hence, Huygens et al. (2008) assume that the $^{15}N$ enrichment in the HF is caused by microbial $^{15}N$ discrimination during nitrogen mineralization and the accumulation of $^{15}N$ enriched microbial components in dense soil fractions. The $^{15}N$ enrichment of the microbial biomass is supposed to happen during plant nitrogen uptake processes through ectomycorrhizal (Huygens et al., 2008). Furthermore, it is to assume that the $^{15}N$ enrichment in mineral-dominated soil fractions is more pronounced if a dominant microbial community is available (Huygens et al., 2008). Therefore, we could speculate that the higher $\delta^{15}N$

signatures and slightly larger isotopic differences between the $\delta^{15}N$ values of the LF and HF were caused due to higher microbial activity at the northern altitudinal gradient.

***$^{13}C$ recovery***

The majority of the south-exposed sites showed balanced $^{13}C$ recoveries among the LF and HF, while the north-facing sites revealed higher $^{13}C$ recoveries in the HF at the forest sites followed by a shift to larger $^{13}C$ recoveries in the LF at the grass-dominated sites. The $^{13}C$ recoveries of both fractions, where dilution of the substrate was considered, showed rising $^{13}C$ recoveries with increasing altitude at the northern gradient (Fig. 34). Meanwhile, the southern gradient (diluted substrate) was characterized by declining $^{13}C$ recoveries with increasing elevation in both density fractions (Fig. 35). Interestingly, the $^{13}C$ recoveries of the forest soils of the northern gradient were very low compared to the $^{13}C$ recoveries at the southern forest sites. The grass dominated higher elevated sites showed inverse $^{13}C$ recoveries. Therefore, the $^{13}C$ recoveries were high at the northern gradient and low at the southern gradient. Furthermore, the $^{13}C$ recoveries of the HF were in some cases (N01, N04 and S07) higher or balanced compared to the $^{13}C$ recoveries of the LF (Fig. 34, Fig. 35). In contrast to these observations, Bird et al. (2008) reported distinctly larger $^{13}C$ recoveries in the LF compared to the HF. However, it is to mention that Bird et al. (2008) did not apply ultrasonic treatment to their samples. Therefore, the LF of Bird et al. (2008) did not contain OC from the occluded fraction, while in our experiment the LF contained the free and occluded fraction. By neglecting dilution of the isotopic signal of the substrate by the natural isotopic composition of the soil, than our $^{13}C$ recoveries of the LF differed from the recoveries of Bird et al. (2008). Bird et al. (2008) recovered in the free LF between 4.9 ± 0.9 % and 14.4 ± 1.4 % of the applied substrate. If dilution of the substrate trough the natural isotopic signature of the soil is considered, then the $^{13}C$ recoveries were in the same range or even higher than Bird et al. (2008) reported. Still, it is to mention that Bird et al. (2008) conducted their density fractionation in the A-horizon. Since Bird et al. (2008) separated only a free light fraction and placed their substrate in the A-horizon, the comparability of the present data with the data from Bird et al. (2008) is limited. Despite this, however, it is difficult to find comparable experiments where similar density fractions were separated and labeled substrate was used to determine fraction-dependent SOC recovery. Therefore, the data of Bird et al. (2008) help to evaluate whether our measurements showed reasonable magnitudes of $^{13}C$ recoveries but an absolute comparison is not possible. However, the $^{13}C$ recoveries of the diluted substrate seem to be more plausible which is why in next chapters only these results will be discussed.

***Fraction-dependent SOC stabilization***

By trend, SOM and degraded SOM of sandy soils can be chemically stabilized in the HF since the HF is most commonly characterized by high soil mass fraction and silt and clay mineral with the potential to chemically interact with organic compounds (Glaser et al., 2000; Hatton et al., 2012; Sollins et al., 2006). The measurements of the present study suggest that a large amount of the added OC is unlikely to have distinct chemical interactions with minerals, since it was found in the LF (Glaser et al., 2000). A smaller amount of the recovered $^{13}C$ was detected in the HF where the potential for chemical binding between OM and minerals is possible. On average, 9.13 ± 3.04 % of the recovered $^{13}C$ (diluted substrate) can be stabilized in the HF at the north-facing sites (Fig. 38). Along the southern gradient, on average 8.33 ± 2.17 % of the recovered $^{13}C$ (diluted substrate) can be stabilized in the soil since it was recovered in the HF (Fig. 38).

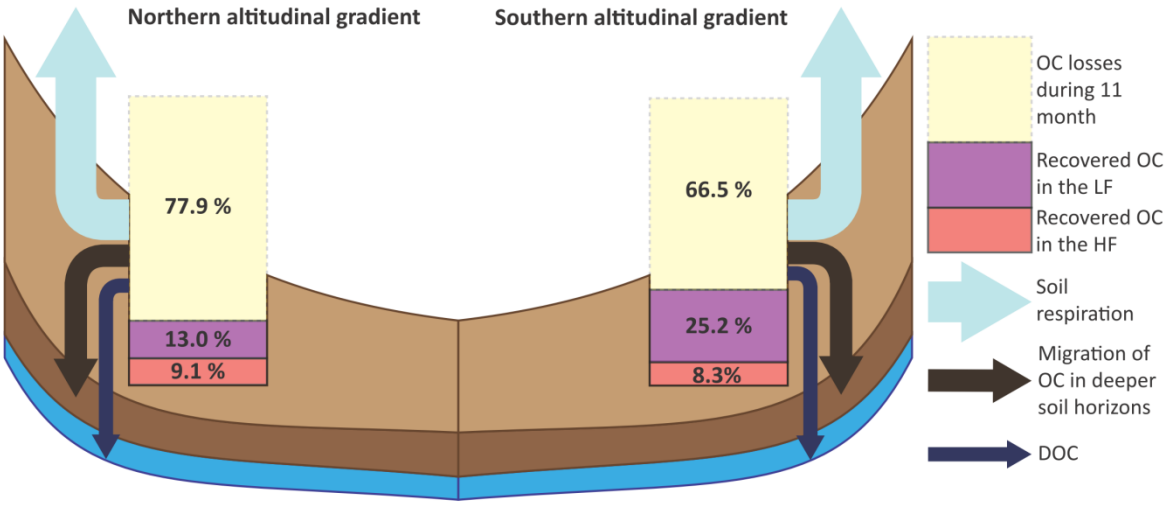


Fig. 38. Mean mass balance of the added substrate at the northern and southern altitudinal gradient (0-5 cm). Organic carbon losses due to soil respiration, migration to deeper soil horizons and dissolved organic carbon (DOC) leaching. Recovered substrate in the light fraction (LF) and heavy fraction (HF).

In agreement with our expectations, the mean value of the recovered and potentially stabilized $^{13}C$ of the HF at the northern gradient exceeded the mean value of the southern gradient. Since the southern gradient showed significantly higher soil temperatures we expected faster SOC decomposition and smaller $^{13}C$ recoveries due to beneficial microbial activity at higher soil temperatures (Davidson et al., 2006). Overall, the balanced and potentially stabilized $^{13}C$ recoveries (diluted substrate) of the northern and southern gradient coincide with observations concerning the mineral contents and mineral-induced protection of SOM from decomposers. For instance, adsorption of SOC onto mineral surfaces through covalent or electrostatic bonds is one protection mechanism (Davidson and Janssens, 2006). Christensen (2001) found beneficial binding capacities for SOC in the silt fraction of sandy soils. Bardelli (2013) reported almost equal amounts of silt and clay in the 0-5 cm soil depth at both gradients. Thus, the similar mineral compositions in the HF of the northern and southern gradient support the balanced $^{13}C$ recoveries along both gradients. However, it would be necessary to investigate the binding characteristics of the recovered $^{13}C$ in the HF by means of nano-scale secondary ion mass spectroscopy to assess the exact stabilization mechanisms of the substrate within organo-mineral clusters (Vogel et al., 2014). Surprisingly, the $^{13}C$ recoveries of the LF at the southern gradient were higher than those at the northern gradient. However, SOC of the LF can be protected within soil aggregates (Davidson and Janssens, 2006; Hatton et al., 2012), which are preferentially found in lower particle densities (<1.6 g $cm^{-3}$) (Cerli et al., 2012). Hence, it could be that the southern gradient exhibited more aggregates in the LF, which protected SOC of the southern gradient from decomposers. Unfortunately, the LF of the present study was not separated into a free light and occluded light fraction and therefore it is not possible to assess whether the SOC of the southern gradient was better protected by soil aggregates from decomposition than the SOC of the northern gradient.

Table 8

Pearson correlation matrix of density fraction specific parameters of the northern gradient (0-5 cm) – bold values indicate significant correlation (p≤0.05), n=5

| | Soil temp. | Sand | Silt | Clay | Difference C/N ratio (LF-HF) | Difference $\delta^{13}C$ (LF-HF) | Difference $\delta^{15}N$ (LF-HF) | $^{13}C$ recovery LF | $^{13}C$ recovery HF | $^{13}C$ recovery LF (diluted substrate) | $^{13}C$ recovery HF (diluted substrate) |
|---|---|---|---|---|---|---|---|---|---|---|---|
| Soil temp. | 1 | 0.06 | 0.62 | 0.35 | 0.68 | -0.47 | -0.21 | -0.86 | -0.49 | **-0.90** | -0.63 |
| Sand | 0.06 | 1 | 0.36 | 0.39 | -0.42 | 0.63 | -0.20 | 0.36 | 0.65 | 0.10 | 0.71 |
| Silt | 0.62 | 0.36 | 1 | 0.84 | 0.43 | -0.10 | 0.34 | -0.57 | -0.39 | -0.56 | -0.29 |
| Clay | 0.35 | 0.39 | 0.84 | 1 | 0.49 | 0.35 | 0.68 | -0.4 | -0.07 | -0.11 | -0.11 |
| Difference C/N ratio (LF-HF) | 0.68 | -0.42 | 0.43 | 0.49 | 1 | -0.32 | 0.43 | **-0.91** | -0.57 | -0.49 | -0.85 |
| Difference $\delta^{13}C$ (LF-HF) | -0.47 | 0.63 | -0.10 | 0.35 | -0.32 | 1 | 0.30 | 0.59 | **0.88** | 0.76 | 0.76 |
| Difference $\delta^{15}N$ (LF-HF) | -0.21 | -0.20 | 0.34 | 0.68 | 0.43 | 0.30 | 1 | -0.17 | -0.16 | 0.34 | -0.19 |
| $^{13}C$ recovery LF | -0.86 | 0.36 | -0.57 | -0.40 | **-0.91** | 0.59 | -0.17 | 1 | 0.76 | 0.79 | **0.91** |
| $^{13}C$ recovery HF | -0.49 | 0.65 | -0.39 | -0.07 | -0.57 | **0.88** | -0.16 | 0.76 | 1 | 0.71 | **0.89** |
| $^{13}C$ recovery LF (diluted substrate) | **-0.90** | 0.10 | -0.56 | -0.11 | -0.49 | 0.76 | 0.34 | 0.79 | 0.71 | 1 | 0.68 |
| $^{13}C$ recovery HF (diluted substrate) | -0.63 | 0.71 | -0.29 | -0.11 | -0.85 | 0.76 | -0.19 | **0.91** | **0.89** | 0.68 | 1 |

Table 9

Pearson correlation matrix of density fraction specific parameters of the southern gradient (0-5 cm) – bold values indicate significant correlation (p≤0.05), n=5

| | Soil temp. | Sand | Silt | Clay | Difference C/N ratio (LF-HF) | Difference $\delta^{13}C$ (LF-HF) | Difference $\delta^{15}N$ (LF-HF) | $^{13}C$ recovery LF | $^{13}C$ recovery HF | $^{13}C$ recovery LF (diluted substrate) | $^{13}C$ recovery HF (diluted substrate) |
|---|---|---|---|---|---|---|---|---|---|---|---|
| Soil temp. | 1 | -0.30 | 0.69 | -0.27 | 0.25 | -0.63 | -0.12 | 0.04 | **0.88** | 0.19 | 0.86 |
| Sand | -0.30 | 1 | 0.05 | -0.72 | 0.27 | -0.24 | -0.81 | **0.90** | 0.11 | 0.38 | 0.04 |
| Silt | 0.69 | 0.05 | 1 | -0.13 | -0.18 | -0.47 | -0.05 | 0.11 | 0.54 | -0.21 | 0.86 |
| Clay | -0.27 | -0.72 | -0.13 | 1 | -0.51 | 0.73 | **0.99** | -0.95 | -0.68 | -0.62 | -0.45 |
| Difference C/N ratio (LF-HF) | 0.25 | 0.27 | -0.18 | -0.51 | 1 | -0.02 | -0.53 | 0.43 | 0.50 | **0.99** | -0.03 |
| Difference $\delta^{13}C$ (LF-HF) | -0.63 | -0.24 | -0.47 | 0.73 | -0.02 | 1 | 0.62 | -0.58 | -0.79 | -0.08 | -0.83 |
| Difference $\delta^{15}N$ (LF-HF) | -0.12 | -0.81 | -0.05 | **0.99** | -0.53 | 0.62 | 1 | **-0.98** | -0.57 | -0.64 | -0.32 |
| $^{13}C$ recovery LF | 0.04 | 0.90 | 0.11 | **-0.95** | 0.43 | -0.58 | **-0.98** | 1 | 0.48 | 0.54 | 0.31 |
| $^{13}C$ recovery HF | **0.88** | 0.11 | 0.54 | -0.68 | 0.50 | -0.79 | -0.57 | 0.48 | 1 | 0.50 | 0.83 |
| $^{13}C$ recovery LF (diluted substrate) | 0.19 | 0.38 | -0.21 | -0.62 | **0.99** | -0.08 | -0.64 | 0.54 | 0.50 | 1 | -0.03 |
| $^{13}C$ recovery HF (diluted substrate) | 0.86 | 0.04 | 0.86 | -0.45 | -0.03 | -0.83 | -0.32 | 0.31 | 0.83 | -0.03 | 1 |

***Gradient-specific $^{13}C$ recoveries***

It is of interest whether the $^{13}C$ recoveries, as an inverse indicator for SOM decomposition, coincide with other decomposition indicating soil properties (density fraction-dependent isotopic characteristics and soil temperature). Therefore, we would like to know whether SOM decomposition indicating soil properties correlate with the $^{13}C$ recoveries along the altitudinal gradients. Interestingly, the $^{13}C$ recoveries of the northern gradient correlate negatively with the soil temperatures (Table 8). This is exactly what Davidson and Janssens (2006) expect for deceasing soil temperature. This trend was significant for the LF of the northern gradient and still observable but not statistical significant for the HF. However, the southern gradient did not show a similar analogy (Table 9). A second approach to evaluate SOM decomposition is to consider the decline (difference) of the C/N ratio between the LF and the HF. Higher differences may indicate stronger decomposition of SOM (Hatton et al., 2012). The north exposed gradient showed a negative correlation between fraction-dependent C/N ratio differences and $^{13}C$ recoveries (Table 8). This can be expected since a pronounced difference in the C/N ratio between density fractions can indicate a high SOM decomposition and, therefore, low $^{13}C$ recoveries. Unfortunately, only the HF of the southern gradient was characterized by a week negative correlation between $^{13}C$ recovery and fraction-dependent C/N ratio differences (Table 9). Another approach to assess SOC decomposition is the consideration of differences in the $\delta^{13}C$ signal of the LF and HF at one sampling site. More pronounced differences in the $\delta^{13}C$ signal between the LF and HF may indicate stronger discrimination of $^{13}C$ against $^{12}C$ during the mineralization of SOC and thus more distinct SOC decomposition and lower $^{13}C$ recoveries (Gunina and Kuzyakov, 2014). Here, the $^{13}C$ recoveries of the southern gradient correlated negatively with the site-specific differences between the $\delta^{13}C$ signal of LF and HF, while the northern gradient did not show similar relations (Table 8, Table 9). Furthermore, the fraction-dependent $\delta^{15}N$ characteristics may help to evaluate the $^{13}C$ recoveries along the altitudinal gradients. Similar to the $^{13}C$ characteristics higher differences in the $\delta^{15}N$ signature of the soil fractions indicate more pronounced SOM decomposition, although $^{15}N$ enrichment in the HF has to be explained by different processes than the $^{13}C$ enrichment. Thus, higher differences between the fraction-specific $\delta^{15}N$ values may indicate distinct SOM decomposition (Huygens et al., 2008). The present data showed an expected negative correlation between the fraction-dependent $\delta^{15}N$ composition and the $^{13}C$ recoveries of the LF and HF at the southern gradient and the HF at the northern gradient (Table 8, Table 9). In sum, it is to mention that the fraction-specific $^{13}C$ recoveries along both altitudinal gradients correlate well with the most decomposition-affine soil properties (fraction-dependent C/N ratio, $\delta^{13}C$ signature and $\delta^{15}N$ composition).

***Exposure-specific $^{13}C$ recoveries***

Furthermore, it is of interest whether the $^{13}C$ recoveries were influenced by exposure. Again the fraction-dependent soil properties can be used to evaluate the $^{13}C$ recoveries. The fraction-dependent differences between isotopic signatures ($\delta^{13}C$) can only explain the higher $^{13}C$ recovery of the HF at the southern northern gradient. The mean value of the fraction-dependent differences between isotopic signatures was distinctly larger at the southern gradient than at the northern gradient (northern gradient: 0.93 ± 0.11 ‰; southern gradient: 1.27 ± 0.06 ‰). Hence, it is to assume that the discrimination of $^{13}C$ against $^{12}C$ was more pronounced at the southern gradient. Therefore, it is to presume that the decomposition of the southern gradient was more pronounced than the decomposition of the northern gradient (Glaser et al., 2000; Powers and Schlesinger, 2002). The

fraction-specific differences between the $\delta^{15}N$ signatures showed similar mean values for both altitudinal gradients. Furthermore, the investigation of the dsDNA, as an indicator for microbial biomass and measured by Bardelli (2013), showed balanced magnitudes for both gradients. Other researcher of the DecAlp project investigated the same sites in Italy with the intention to analyze the microbial community along the climosequence. Gómez-Brandón et al. (2014), for instance, identified and quantified soil biota along the climosequence. They found more microannelids and bacteria at the southern altitudinal gradient. These observations coincide with observations from Bardelli (2013). Furthermore, the more acidic pH values of the northern gradient may indicate lower SOM decomposition at the north-facing sites (Leifeld et al., 2013). In sum, it is to mention that the soil temperature, the soil pH and the fraction-dependent isotopic abundances indicate preferential conditions for SOM decomposition at the southern gradient. The $^{13}C$ recoveries of the HF coincide with these observations (lower $^{13}C$ recoveries in the HF at the southern gradient), while the $^{13}C$ recoveries of the LF did not follow this trend. However, the present study did not investigate the mineral composition of the soil sample, soil moisture or aggregate formation in the LF. Hence, further analysis about the free and occluded light fraction of the soil fraction ≤1.6 g $cm^{-3}$ and the investigation of the soil moisture may help to explain the exposure-specific $^{13}C$ recoveries of the LF.

# 5 Conclusion

In conclusion, the experiments have shown that both elevation gradients were characterized by heterogeneous soil properties, substrate decomposition and stabilization mechanisms. This demonstrated that Alpine sites are exposed to extreme climatic conditions and also explains the heterogeneity of the present data. Nevertheless, exposure und elevation-specific trends could be observed along the climosequence in the northern Italian Alps. The following general findings were obtained:

- The SOC concentration and C/N ratio of the bulk showed a clear trend from forest-dominated values to grassland-dominated values. This means that the SOC concentration and the C/N ratio were altered by elevation. Despite this, the SOC concentration, nitrogen concentration and the C/N ratio of the bulk soil were not significantly affected by exposure.
- The SOC stocks of the bulk soil (0-15 cm) showed balanced magnitudes among the northern and southern altitudinal gradient. Nevertheless, the SOC stocks developed differently along the gradients. At the northern gradient maximum SOC stocks were reached at the timberline and stayed constant at higher elevated sites. Meanwhile, the SOC stocks of the southern gradient rose continuously with increasing altitude.
- The investigation of the density fractions (0-5 cm) resulted in the finding that distinct amounts of the soil mass were recovered in the heavy fraction (HF). Meanwhile the light fraction (LF) was characterized by significant SOC and nitrogen concentrations. Furthermore, the soil parameters SOC concentration, nitrogen concentration, C/N ratio were characterized by decreasing magnitudes with increasing fraction density. The $\delta^{13}C$ and the $\delta^{15}N$ values rose with increasing particle density.
- The C/N ratios of the bulk soil as well as the fraction-dependent C/N ratios, the fraction-specific $\delta^{13}C$ signatures, the fraction-dependent $\delta^{15}N$ compositions, the soil temperatures and the soil pH indicate preferential SOM decomposition conditions at the southern altitudinal gradient.
- The $^{13}C$ recovery (as the inverse indicator for SOM decomposition) of the bulk soil showed for the southern gradient slightly but not significantly higher $^{13}C$ recoveries than at the northern gradient. Similar regimes were observed for the $^{13}C$ recoveries of the LF. However, the $^{13}C$ recoveries of the HF followed the expected pattern of lower $^{13}C$ reveries at the southern gradient. The $^{13}C$ recoveries exhibited rising recoveries with increasing altitude at the northern gradient, whereas the $^{13}C$ recoveries at the southern gradient declined with increasing altitude.
- On average, approximately 9 % of the applied substrate was recovered in the mineral-dominated soil fraction (HF). This recovered substrate of the HF can potentially be stabilized in the soil due to interactions with reactive mineral surfaces. The stabilization because of aggregate formation was not investigated.

The investigation of this considerable climosequence (different exposures and extensive investigation of different altitudes) resulted in a fundamental understanding of soil processes as a function of climatic conditions in an alpine environment. Temperature and precipitation seem to be crucial for the soil processes and parameters in an alpine ecosystem. Especially SOM decomposition, as one important factor in the global carbon cycle, showed a distinct sensitivity due to temperature and precipitation changes along the climosequence. On the basis of this knowledge further analysis concerning the effect of climate warming in alpine region would be possible.

# 6 Acknowledgment

Special thanks go to Prof. Markus Egli and Dr. Samuel Abiven for their helpful and target-oriented support at any point of time during the process of this master thesis. Furthermore, I would like to thank to the University of Zurich, especially to Sandra Röthlisberger and Michael Hilf who enabled me to conduct all laboratory analyses. Further thanks also go to the ZHAW Life Science and Facility Management and the Fodanzione Edmund Mach (FEM), which conducted several measurements used in the present thesis. Then I would also like to give thanks to Claudia Neuhaus, Sandra Gut and Dieter Halpern for the professional suggestions and corrections concerning the present master thesis.

# 7 Literature


Bardelli, T., 2013. Impatto di differenti sequenze microclimatiche (altitudine, esposizione) sulle caratteristiche fisico-chimiche e microbiologiche di suoli alpini (Trentino Alto Adige). Universita Degli Studi Firenze.

Bernoux, M., Cerri, C.C., Neill, C., de Moraes, J.F.., 1998. The use of stable carbon isotopes for estimating soil organic matter turnover rates. Geoderma 82, 43–58.

Bird, J.A., Kleber, M., Torn, M.S., 2008. $^{13}C$ and $^{15}N$ stabilization dynamics in soil organic matter fractions during needle and fine root decomposition. Organic Geochemistry 39, 465–477.

Bottner, P., Coûteaux, M.M., Anderson, J.M., Berg, B., Billès, G., Bolger, T., Casabianca, H., Romanyá, J., Rovira, P., 2000. Decomposition of $^{13}C$-labelled plant material in a European 65-40° latitudinal transect of coniferous forest soils: Simulation of climate change by translocation of soils. Soil Biology and Biochemistry 32, 527–543.

Cerli, C., Celi, L., Kalbitz, K., Guggenberger, G., Kaiser, K., 2012. Separation of light and heavy organic matter fractions in soil - Testing for proper density cut-off and dispersion level. Geoderma 170, 403–416.

Christensen, B., 1992. Physical Fractionation of Soil and Organic Matter in Primary Particle Size and Density Separates. In: Stewart, B.A. (Ed.), Advances in Soil Science. Springer New York, pp. 1–90.

Christensen, B.T., 2001. Physical fractionation of soil and structural and functional complexity in organic matter turnover. European Journal of Soil Science 52, 345–353.

Dahlgren, R.A., Rasmussen, C., Southard, R.J., 1997. Soil development along elevational transects on granite , andesitic lahar and basalt in the western Sierra Nevada , California. Geoderma 78, 207–236.

Dalmolin, R.S.D., Gonçalves, C.N., Dick, D.P., Knicker, H., Klamt, E., Kögel-Knabner, I., 2006. Organic matter characteristics and distribution in Ferralsol profiles of a climosequence in southern Brazil. European Journal of Soil Science 57, 644–654.

Davidson, E.A., Janssens, I.A., 2006. Temperature sensitivity of soil carbon decomposition and feedbacks to climate change. Nature 440, 165–173.

Davidson, E.A., Janssens, I.A.., Lou, Y., 2006. On the variability of respiration in terrestrial ecosystems: Moving beyond Q10. Global Change Biology 12, 154–164.

Djukic, I., Zehetner, F., Tatzber, M., Gerzabek, M.H., 2010. Soil organic-matter stocks and characteristics along an alpine elevation gradient. Journal of Plant Nutrition and Soil Science 173, 30–38.

Egli, M., Fitze, P., 2001. Quantitative aspects of carbonate leaching of soils with differing ages and climates. Catena 46, 35–62.

Egli, M., Mirabella, A., Sartori, G., Zanelli, R., Bischof, S., 2006. Effect of north and south exposure on weathering rates and clay mineral formation in Alpine soils. Catena 67, 155–174.

Egli, M., Sartori, G., Mirabella, A., Favilli, F., Giaccai, D., Delbos, E., 2009. Effect of north and south exposure on organic matter in high Alpine soils. Geoderma 149, 124–136.

Fontaine, S., Bardoux, G., Benest, D., Verdier, B., Mariotti, A., Abbadie, L., 2004. Mechanisms of the Priming Effect in a Savannah Soil Amended with Cellulose. Soil Science Society of America Journal 68, 125–131.

Garcia-Pausas, J., Casals, P., Camarero, L., Huguet, C., Sebastià, M.T., Thompson, R., Romanyà, J., 2007. Soil organic carbon storage in mountain grasslands of the Pyrenees: Effects of climate and topography. Biogeochemistry 82, 279–289.

Garten, C.T.J., Cooper, L.W., Post, W.M., Hanson, P.J., 2000. Climate controls on forest soil C isotope ratios in the southern appalachian mountains. Ecology 81, 1108–1119.

Garten, C.T.J., Hanson, P.J., 2006. Measured forest soil C stocks and estimated turnover times along an elevation gradient. Geoderma 136, 342–352.

Garten, C.T.J., Post, W.M., Hanson, P.J., Cooper, L.W., 1999. Forest soil carbon inventories and dynamics along an elevation gradient in the southern Appalachian Mountains. Biogeochemistry 45, 115–145.

Glaser, B., Balashov, E., Haumaier, L., Guggenberger, G., Zech, W., 2000. Black carbon in density fractions of anthropogenic soils of the Brazilian Amazon region. Organic Geochemistry 31, 669–678.

Gómez-Brandón, M., Ascher, J., Bardelli, T., Beylich, A., Egli, M., Pietramellara, G., Sartori, G., Insam, H., Graefe, U., 2014. Interactive effects of altitude and exposure on soil biota in different Alpine vegetation zones, In: First Global Soil Biodiversity Conference 2014, 2nd-5th December, Dijon, France.

Gruber, S., Hoelzle, M., Haeberli, W., 2004. Rock-wall temperatures in the Alps: Modelling their topographic distribution and regional differences. Permafrost and Periglacial Processes 15, 299–307.

Gunina, A., Kuzyakov, Y., 2014. Pathways of litter C by formation of aggregates and SOM density fractions: Implications from $^{13}C$ natural abundance. Soil Biology and Biochemistry 71, 95–104.

Harmon, M.E., Franklin, J.F., Swanson, F.J., Sollins, P., Gregory, S. V., Lattin, J.D., Anderson, N.H., Cline, S.P., Aumen, N.G., Sedell, J.R., Lienkaemper, G.W., Cromack, Jr., K., Cummins, K.W., 1986. Ecology of Coarse Woody Debris in Temperate Ecosystems. Advances in Ecological Reseacrch 15, 133–276.

Hatton, P.J., Kleber, M., Zeller, B., Moni, C., Plante, A.F., Townsend, K., Gelhaye, L., Lajtha, K., Derrien, D., 2012. Transfer of litter-derived N to soil mineral-organic associations: Evidence from decadal $^{15}N$ tracer experiments. Organic Geochemistry 42, 1489–1501.

Hitz, C., Egli, M., Fitze, P., 2001. Below-ground and above-ground production of vegetational organic matter along a climosequence in alpine grasslands. Journal of Plant Nutrition and Soil Science 164, 389–397.

Hultine, K.R., Marshall, J.D., 2000. Altitude trends in conifer leaf morphology and stable carbon isotope composition. Oecologia 123, 32–40.

Huygens, D., Denef, K., Vandeweyer, R., Godoy, R., Van Cleemput, O., Boeckx, P., 2008. Do nitrogen isotope patterns reflect microbial colonization of soil organic matter fractions? Biology and Fertility of Soils 44, 955–964.

Jenny, H., Gessel, S.P., Bingham, F.T., 1949. Comparative study of decomposition rates of organic matter in temperate and tropical regions. Soil Science 68, 419–432.

Kammer, A., Hagedorn, F., 2011. Mineralisation, leaching and stabilisation of $^{13}$C-labelled leaf and twig litter in a beech forest soil. Biogeosciences 8, 2195–2208.

Kirschbaum, M.U., 1995. The temperature dependence of soil organic matter decomposition, and the effect of global warming on soil organic C storage. Soil Biology and Biochemistry 27, 753–760.

Kleber, M., Sollins, P., Sutton, R., 2007. A conceptual model of organo-mineral interactions in soils: Self-assembly of organic molecular fragments into zonal structures on mineral surfaces. Biogeochemistry 85, 9–24.

Kragten, J., 1994. Calculating Standard Deviations and Confidence Intervals with a Universally Applicable Spreadsheet Technique. Analyst 119, 2161–2165.

Kueppers, L.M., Harte, J., 2005. Subalpine forest carbon cycling: short-and long-term influence of climate and species. Ecological Applications 15, 1984–1999.

Kuzyakov, Y., Friedel, J.K., Stahr, K., 2000. Review of mechanisms and quantification of priming effects. Soil Biology & Biochemistry 32, 1485–1498.

Leifeld, J., Bassin, S., Conen, F., Hajdas, I., Egli, M., Fuhrer, J., 2013. Control of soil pH on turnover of belowground organic matter in subalpine grassland. Biogeochemistry 112, 59–69.

Leifeld, J., Zimmermann, M., Fuhrer, J., Conen, F., 2009. Storage and turnover of carbon in grassland soils along an elevation gradient in the Swiss Alps. Global Change Biology 15, 668–679.

Liski, J., Nissinen, a, Erhard, M., Taskinen, O., 2003. Climatic effects on litter decomposition from arctic tundra to tropical rainforest. Global Change Biology 9, 575–584.

Lorenz, K., Preston, C.M., Raspe, S., Morrison, I.K., Feger, K.H., 2000. Litter decomposition and humus characteristics in Canadian and German spruce ecosystems: Information from tannin analysis and $^{13}$C CPMAS NMR. Soil Biology and Biochemistry 32, 779–792.

Malhi, Y., 2002. Carbon in the atmosphere and terrestrial biosphere in the 21st century. Philosophical transactions. Series A, Mathematical, physical, and engineering sciences 360, 2925–45.

Marrs, A.R.H., Proctor, J., Heaney, A., Mountford, M.D., Marrs, R.H., Experimental, M.W., 1988. Changes in Soil Nitrogen-Mineralization and Nitrification Along an Altitudinal Transect in Tropical Rain Forest in Costa Rica. Jurnal of Ecology 76, 466–482.

Meentemeyer, V., Box, E.O., Thompson, R., 1982. World Patterns and Litter Amounts of Terrestrial Plant Production. BioScience 32, 125–128.

Murphy, K.L., Klopatek, J.M., Klopatek, C.C., Applications, S.E., Nov, N., Klopatek, C.C.O.E., 1998. The Effects of Litter Quality and Climate on Decomposition along an Elevational Gradient. Ecoligical applications 8, 1061–1071.

Petrillo, M., Cherubini, P., Sartori, G., Abiven, S., Ascher, J., Bertoldi, D., Camin, F., Barbero, A., Larcher, R., Egli, M., 2015. Decomposition of Norway spruce and European larch coarse woody debris (CWD) in realtion to different elevation and exposure in an Alpine setting. iForest in press.

Powers, J.S., Schlesinger, W.H., 2002. Geographic and vertical patterns of stable carbon isotopes in tropical rain forest soils of Costa Rica. Geoderma 109, 141–160.

Powers, R.F., 1990. Nitrogen mineralization along an altitudinal gradient: Interactions of soil temperature, moisture, and substrate quality. Forest Ecology and Management 30, 19–29.

Rodeghiero, M., Cescatti, A., 2005. Main determinants of forest soil respiration along an elevation/temperature gradient in the Italian Alps. Global Change Biology 11, 1024–1041.

Rubino, M., Dungait, J. a J., Evershed, R.P., Bertolini, T., De Angelis, P., D'Onofrio, a., Lagomarsino, a., Lubritto, C., Merola, a., Terrasi, F., Cotrufo, M.F., 2010. Carbon input belowground is the major C flux contributing to leaf litter mass loss: Evidences from a $^{13}C$ labelled-leaf litter experiment. Soil Biology and Biochemistry 42, 1009–1016.

Schaetzl, R., Anderson, S., 2005. Soils: Genesis and Geomorphology. Cambridge University Press.

Schindlbacher, A., De Gonzalo, C., Díaz-Pinés, E., Gíorra, P., Matthews, B., Inclán, R., Zechmeister-Boltenstern, S., Rubio, A., Jandl, R., 2010. Temperature sensitivity of forest soil organic matter decomposition along two elevation gradients. Journal of Geophysical Research: Biogeosciences 115, 1–10.

Schmid, M.O., Gubler, S., Fiddes, J., Gruber, S., 2004. Inferring snowpack ripening and melt-out from distributed measurements of near-surface ground temperatures. Soil Science Society of America Journal 68, 125–131.

Schmidt, M.W.I., Rumpel, C., Kögel-Knabner, I., 1999. Evaluation of an ultrasonic dispersion procedure to isolate primary organomineral complexes from soils. European Journal of Soil Science 50, 87–94.

Schmidt, M.W.I., Torn, M.S., Abiven, S., Dittmar, T., Guggenberger, G., Janssens, I. a, Kleber, M., Kögel-Knabner, I., Lehmann, J., Manning, D. a C., Nannipieri, P., Rasse, D.P., Weiner, S., Trumbore, S.E., 2011. Persistence of soil organic matter as an ecosystem property. Nature 478, 49–56.

Schrumpf, M., Kaiser, K., Guggenberger, G., Persson, T., Kögel-Knabner, I., Schulze, E.D., 2013. Storage and stability of organic carbon in soils as related to depth, occlusion within aggregates, and attachment to minerals. Biogeosciences 10, 1675–1691.

Sierra, C.A., 2012. Temperature sensitivity of organic matter decomposition in the Arrhenius equation: Some theoretical considerations. Biogeochemistry 108, 1–15.

Singh, N., Abiven, S., Maestrini, B., Bird, J.A., Torn, M.S., Schmidt, M.W.I., 2014. Transformation and stabilization of pyrogenic organic matter in a temperate forest field experiment. Global Change Biology 20, 1629–1642.

Sollins, P., Swanston, C., Kleber, M., Filley, T., Kramer, M., Crow, S., Caldwell, B. a., Lajtha, K., Bowden, R., 2006. Organic C and N stabilization in a forest soil: Evidence from sequential density fractionation. Soil Biology and Biochemistry 38, 3313–3324.

Stahr, K., Kandeler, E., Herrmann, L., Streck, T., 2012. Bodenkunde und Standortlehre: Grundwissen Bachelor, 2nd ed. Eugen Ulmer Stuttgart, Stuttgart.

Vogel, C., Mueller, C.W., Höschen, C., Buegger, F., Heister, K., Schulz, S., Schloter, M., Kögel-Knabner, I., 2014. Submicron structures provide preferential spots for carbon and nitrogen sequestration in soils. Nature communications 5, 2947.

Von Lützow, M., Kögel-Knabner, I., Ekschmitt, K., Flessa, H., Guggenberger, G., Matzner, E., Marschner, B., 2007. SOM fractionation methods: Relevance to functional pools and to stabilization mechanisms. Soil Biology and Biochemistry 39, 2183–2207.

Wagai, R., Mayer, L.M., Kitayama, K., Knicker, H., 2008. Climate and parent material controls on organic matter storage in surface soils: A three-pool, density-separation approach. Geoderma 147, 23–33.

Weedon, J.T., Cornwell, W.K., Cornelissen, J.H.C., Zanne, A.E., Wirth, C., Coomes, D.A., 2009. Global meta-analysis of wood decomposition rates: A role for trait variation among tree species? Ecology Letters 12, 45–56.

Zollinger, B., Alewell, C., Kneisel, C., Meusburger, K., Gärtner, H., Brandová, D., Ivy-Ochs, S., Schmidt, M.W.I., Egli, M., 2013. Effect of permafrost on the formation of soil organic carbon pools and their physical-chemical properties in the Eastern Swiss Alps. Catena 110, 70–85.

# 8 Appendix

## R-Code for the Piccaro evaluation:

```
matrix1=read.csv("C:/Users/Simon/Documents/R/data2.csv", header=TRUE, sep=";")
thd1=0.2                                                    #set threshold1 (thd1= threshold 1 first derivation
                                                            #(here optimal at 0.2))
thd2=-380                                                   #set threshold2 (thd2= threshold 2 second derivation)
CO2=matrix1[ ,19]                                           #VERRY IMPORTANT TO CHECK: column of 12CO2
y=length(CO2)
t=as.character(matrix1[,2])
d=as.Date(matrix1[,1], "%d.%m.%Y")
t1<-times(t)
t2<-matrix1[,3]

s1=c()
for(i in 1:y)
{
 s1[i]=(t2[i+1]-t2[i])*24*3600
 s1[y]=0.5*(s1[y-1]+s1[y-2])
}
s2=mean(s1)
stdv=sd(s1)
m=c()
for(i in 1:y)                                               #first numeric derivation of CO2
{
 m[i]=((CO2[i+1]-CO2[i])/(t2[i+1]-t2[i])+((CO2[i]-CO2[i-1])/(t2[i]-t2[i-1])))/(t2[i+1]-t2[i-1])
 m[1]=0.5*(m[2]+m[3])
 m[y]=0.5*(m[y-1]+m[y-2])
}
k=c()                                                       #k=second numeric derivation of CO2
for (i in 1:y)
{
 k[i]=((CO2[i+1]-CO2[i])+(CO2[i]-CO2[i-1])-2*CO2[i])/(1/3*(s1[i+1]+s1[i]+s1[i-1]))^2
 k[1]=0.5*(k[2]+k[3])
 k[y]=0.5*(k[y-1]+k[y-2])
}
k1=c()
sep=c()
sep1=c()                                                    #intermediate step to achieve sep2
sep2=c()                                                    #final separation vector [0,1] with 0=background CO2, 1 = CO2 signal sample
graph1=c()
for (i in 1:y)                                              #all conditions for definition start and end of CO2 peak
{
 k1[i]=(s1[i+2]*k[i+2]+s1[i+1]*k[i+1]+s1[i]*k[i]+s1[i-1]*k[i-1]+s1[i-2]*k[i-2])/
          (s1[i+2]+s1[i+1]+s1[i]+s1[i-1]+s1[i-2])    #smoothing of second derivation for better results
 k1[1]=0.5*(k1[2]+k[3])
 k1[y]=0.5*(k1[y-1]+k[y-2])
 sep[i]=ifelse(sqrt((m[i])^2)<=thd1, m[i]*0, m[i]^0)        #first condition: slop
 sep1[i]=ifelse(sep[i]==0 & k1[i]<=thd2, sep[i]^0, sep[i]*1)    #second condition: second derivation at local maximum
 sep2[i]=ifelse(sqrt((m[i])^2)>=thd1 & k1[i]>thd2, sep1[i]*0, sep1[i]*1)    #third condition: eliminate single
                                                            #values of background noise
 sep2[1]=sep2[2]
 graph1[i]=ifelse(sep2[i]==1, sep2[i]*1, sep2[i]*NA)
}
sepop=c()                                                   #sepop=opposite of sep2 [0,1] with 1 = background CO2 and 0 = CO2 signal sample
for(i in 1:y)
{
 sepop[i]=ifelse(sep2[i]==0, sep2[i]^0, sep2[i]*NA)
}
CO2bg=CO2*sepop                                             #CO2bg= CO2 background
meanCO2bg=mean(CO2bg, na.rm=TRUE)                           #meanCO2bg= mean value of CO2 background signal
stdvCO2bg=sd(CO2bg, na.rm=TRUE)                             #stdvCO2bg= standard deviation of CO2 background signal
CO2c=CO2-meanCO2bg                                          #CO2c= CO2 signal sample minus CO2 background
CO2sample=sep2*CO2c*s1                                      #CO2sample= final CO2 value per time step


plot(t1,CO2sample, pch=20, lwd=0.01, col=ifelse(CO2sample>0, "red", "black"))
                                                            #where the red dots are--> CO2 signal will be summed up
```

```
sep3=c()                                    #sep3= separation 3, will be used to define number of CO2 peaks of    #the samples
for(i in 1:y)
{
 sep3[i]=ifelse(sep2[i]-sep2[(i-1)]>0, sep[i]*1,sep[i]*0)
                                            #find step changes from 0 to 1 in sep2 which represents the start of   #CO2 signal of
the sample
}
r=c(0,NA)
idx= which(sep3 %in% r)
sep4=sep3[-idx]                             #find automatically step changes in sep3
n=length(sep4)                              #n= number of step changes-->number of CO2 signal form sample

r1=c(1)
idx1= which(sep3 %in% r1)                   #find position of step change in sep3

CO2sample1=c()
for(i in 1:y)                               #killing NA and replace by 0 -->last value of y will be zero (problem if signal is not completely
finished)
{
 CO2sample1[i]=ifelse(is.na(CO2sample[i]), (CO2sample[i]^0)*0, CO2sample[i]*1)
}


z<-matrix(nrow=n,ncol=y)                    #z= new matrix to save CO2 signal of each sample
for(i in 1:n)
{
 j=idx1[i]
 while (CO2sample1[j]>0)
 {
  z[i,j]=(CO2sample1[j])
  j=j+1
 }
}


number=c()
CO2.tot=c()
integral.length=c()
time=matrix1[,2]
start=c()

kill=c()
for (i in 1:n)
{
 number[i]=i
 CO2.tot[i]=sum(z[i,],na.rm=TRUE)
 integral.length[i]=sum(z[i,]/z[i,], na.rm=TRUE)
 start[i]=as.character(time[idx1[i]])
}

sCO2ps<-data.frame(number, CO2.tot, integral.length, start)
sCO2ps1<-data.frame(number, CO2.tot, integral.length, start)
for(i in 1:n)
 {
 if(sCO2ps[i,3]<=20)
{
 sCO2ps1[-i,]
}
}
quality_levels<-data.frame(meanCO2bg, stdvCO2bg)
print(sCO2ps1)
print(quality_levels)
```

Personal declaration: I hereby declare that the submitted thesis is the result of my own, independent work. All external sources are explicitly acknowledged in the thesis.